nature portfolio

Peer Review File

Targeting a Super-Enhancer induced Aldehyde Dehydrogenase metabolic loop mitigates CDK4/6 Inhibitor Resistance in Estrogen Receptor-Positive Cancers

Corresponding Author: Dr Zhaoliang Yu

This file contains all reviewer reports in order by version, followed by all author rebuttals in order by version.

Version 0:

Reviewer comments:

Reviewer #1

(Remarks to the Author)
In this study, Chen and colleagues investigated the effects of abnormal ALDH1A1 expression on CDK4/6i resistance in hormone receptor-positive breast and endometrial cancers. The researchers demonstrate that high ALDH1A1 levels and their downstream effects contribute to CDK4/6i insensitivity.
We have some comments:
1) The methodology used for the sensitivity profiling of abemaciclib against 16 PDOs from EC is unclear. How do other CDK4/6 inhibitors such as Palbociclib and Ribociclib compare? Is the response CDK4- or CDK6-specific?
2) What dose is considered the threshold for Abemaciclib resistance in vitro? In Supplementary Figure 2, the authors show response curves from a wide variety of endometrial cancer cells. Indicating IC50 values would increase the interpretability of the results.
3) Quantification and replicates of analyses in Figure 3, as the effects of knockdown, overexpression of ALDH1A1 or its inhibition, and others throughout the manuscript seem to be missing.
Moreover, in the manuscript, considerable amount of conclusions were drawn from visual data, such as colony formation assays and immunofluorescence / immunohistochemistry. Although they might still convey the main idea, the quality of the visuals is low, making a through revision challenging. It is essential that the manuscript includes either significantly improved visuals or clear, detailed quantitative data to support the findings. As an example, in Figure 2K, although the difference is clear, the cells in the resistance group look rather overexposed, very likely due to image quality. Additionally, immunofluorescence images should include a legend indicating the color assigned to each marker.
4) The ChIP-seq data and others don't seem to be available for review. Has it been uploaded to a repository? No quality metrics seem to be provided. What where the controls in these experiments?
5) In the experiments shown in Figure 4A and Figure 6M, the authors indicate that they treat the cells with 20 µM ATRA. In our experience this is way over the relevant in vitro therapeutic dose, which is conventionally between 0.01-1 µM. This is also valid for Vitamin A treatments - the authors should test if the effects of RA and Vitamin A are dose-dependent, in order to ensure that very high doses are not skewing the responses away from what is physiologically and therapeutically relevant.
6) In Figure 2J, what do P1, 2, 3, and 4 correspond to? In the legend it was stated that the data was shown as mean ± SD of technical triplicates. If they are biological replicates, it would be more sensible to show the cumulative data as n=4 and perform statistics. Moreover, the graph type that was chosen is not suitable for a t-test.
In general, the number of biological replicates seems not to be indicated in all of the experiments, so the authors should provide this information.
7) Throughout the manuscript, some data were shown as mean ± SD, while some were shown as mean ± SEM (although authors only stated it as ± SEM, which needs additional correction). The data presentation must follow a uniform format to ensure clarity and consistency across the manuscript.
8) The authors established 4 Abemaciclib resistant cell models with HEC-1-A, HEC-1-B, MCF7 and T47D cells through chronic exposure. Figure 2A indicates that they used increasing doses of Abemaciclib, while DMSO seems to be constant. In our experience DMSO itself might have substantial effect on the cells. Was DMSO amount also increased in parallel? The authors should describe the establishment of their acquired resistance models in more detail.
9) The authors had 8 EC cells lines at the hand, why did they choose to move forward with HEC-1-A and HEC-1-B cells, since HEC-1-B is the substrain of HEC-1-A cells and therefore very similar? Wouldn't a more distinct cell model be preferable?

10) In Figure 1J, the authors show enrichment of epithelial mesenchymal transition (EMT), KRAS and estrogen response signaling in resistant tumors, not surprisingly so, considering KRAS is known to be frequently mutated in Type I endometrial EC, which represents 87.50% of the cohort of the study. Can authors provide information regarding KRAS status of their patient cohort? Could KRAS activating mutations already be an indication of resistance? The same question also stands for the dataset they use for T47D palbociclib resistance model - KRAS is also highly expressed in T47D. Could the palbociclib treatment select the cells with strong KRAS signaling and have increased EMT features? Notably, given that these pathways appear critical to their resistance models, how might the authors relate this to their current findings? Does KRAS activation favor higher ALDH1A1 activity as well? Additionally, as EMT was shown to be a key feature of Abemaciclib resistance, did authors observe any change in the EMT features in their ALDH1A1 overexpression / silencing models? These points should be more clearly integrated into the manuscript to strengthen the overall narrative of the work.
11) In lines 144-146, authors state that their histological analyses showed morphological similarities between PDOs and their corresponding primary EC tumors. However, PDOs exhibited great distinction in sensitivity to CDK4/6i Abemaciclib. In its current form, the sentence implies that authors tested Abemaciclib sensitivity of tumors before the PDOs were formed and there is a difference after PDO formation. If this was done, the authors should show the data and discuss the potential mechanisms. If not, the sentence should be revised.
12) For experiments with viral transduction, such as in Figure 3D, comparisons focus on control groups, but the relationship between empty vector controls and parental cells is not addressed.
13) In Figure 4H, the scatter diagrams show the IC50 of Palbociclib in GDSC database between high and low activation of vitA metabolic, RA signaling, RA metabolic and RA nuclear binding. This is particularly interesting, considering CDK4/6i such as palbociclib are considered candidate drugs to be used in combination for differentiation therapy in cancers such as acute myeloid leukemia and neuroblastoma (PMID: 37734383, PMID: 38507743). For the comprehensiveness of the study, it would be beneficial for the authors to address this discrepancy in the discussion.
14) In the study, after conducting extensive experiments, the authors identified the BRD4 inhibitor dBET6 as the most potent Abemaciclib sensitizer. While the data leading to this conclusion is solid, BET inhibitors were previously shown target ALDH1A1 super-enhancer in a 2016 work by Yokoyama & Zhu et al. (PMID: 27803105), which authors actually referenced in line 205 (Reference number 35), only to state that ALDH1A1 was a gene that was previously reported to be associated with chemoresistance. Although the two works focus on different cancer types, there are methods and conclusions that seem parallel; this should be addressed and discussed accordingly.
15) In Line 338: “Additionally, functional studies showed that genetic deletion of RARα
339 with siRNAs...” Deletion is not the correct term for siRNA.
16) In the study, substantial portion of experimental results were reported as technical replicates and yet, authors performed statistics and made certain conclusions. Since authors also showed in some the data (such as in Figure 3E) where they actually had three biological replicates, the term “technical replicates” implies that some of the experiments were performed only once, with technical replicates. The authors should either reach the number of enough biological replicates before performing statistics or correct the manuscript if it is a typographical error.
The list of experiments where only technical replicates were shown;
-Figure 2I; lines 1148-1150 in the legend: “RT-qPCR validation of ALDH1A1 in parental and resistant cells. Data are shown as mean ± SD of technical triplicates and analyzed by unpaired t-test”
-Figure 2J; lines 1152-1152 in the legend: Data are presented relative to input, shown as mean ± SD of technical triplicates and analyzed by unpaired t-test.
-Figure 3K; lines 1188-1192 in the legend: Representative images of PDO67, PDO76 and PDO77 treated with DMSO, Abemaciclib (1 μM), Dis (2 μM), dBET6 (2 μM), or combination after 10 days culture. Scale bar = 200 μm (left). The matching scatter diagram shows data as mean ± SD of technical triplicates, ***$p < 0.001$, one-way ANOVA with Dunnett’s multiple comparisons test (right).
-Figure 4B: lines 1196-1199 in the legend: Determination of relative RA concentrations between parental cells (HEC-1-AP and HEC-1-BP) and resistant cells (HEC-1-AR and HEC-1-BR). Data are shown as mean ± SD of technical triplicates and analyzed by unpaired t-test.
-Figure 4C: lines 1199-1202 in the figure legend: Determination of relative vitA concentrations in cell culture medium at the indicated time points. Data are shown as mean ± SD of technical triplicates and analyzed by two-way ANOVA with Dunnett’s multiple comparisons test, ***$p < 0.001$.
-Figure 4G; lines 1208-1212 in the figure legend: Resistant cells are treated with the indicated concentrations of Abemaciclib in B-27 supplement medium, vitA-deficient B-27 supplement medium or vitA-deficient B-27 supplement medium with vitA (10 μM). The number of viable cells is measured at 96 hours. Data are shown as mean ± SD of technical triplicates and analyzed by two-way ANOVA with Dunnett’s multiple comparisons test, ***$p < 0.001$.
-Figure 4J; lines 1216-1218 in the figure legend: Relative ALDH enzyme activity between parental cells (HEC-1-AP and HEC-1-BP) and resistant cells (HEC-1-AR and HEC-1-BR). Data are shown as mean ± SD of technical triplicates and analyzed by unpaired t-test.
-Figure 4L; lines 1219-1221 in the figure legend: Relative ALDH enzyme activity of indicated cells. Data are shown as mean ± SD of technical triplicates and analyzed by One-way ANOVA with Dunnett’s multiple comparisons test.
-Figure 4N; lines 1223-1225 in the figure legend: Determination of relative RA concentrations in indicated cells. Data are shown as mean ± SD of technical triplicates and analyzed by one-way ANOVA with Dunnett’s multiple comparisons test.
-Figure 4O; Determination of relative RA concentrations in cells transfected with siNC or siALDH1A1. Data are shown as mean ± SD of technical triplicates and analyzed by unpaired t-test. ****$p < 0.0001$.
-Figure 5J; lines 1248-1252 in the figure legend; Representative images of PDO77, PDO76 and PDO80 treated with DMSO, Abemaciclib (1 μM), AGN (20 μM), AR7 (20 μM), or combination after 10 days culture (left). Scale bar = 200 μm. The matching scatter diagram shows data as mean ± SD of technical triplicates, one-way ANOVA with Dunnett’s multiple comparisons test (right). **$p < 0.01$, ***$p < 0.001$, ****$p < 0.0001$.
-Figure 6F-G; lines 1265-1267 in the figure legend; ChIP-qPCR analysis of RARα and ERα occupancy at genomic loci of ALDH1A1 in HEC-1-AP and HEC-1-AR, HEC-1-BP and HEC-1-BR cells. Data are presented relative to input, shown as

mean ± SD of technical triplicates and analyzed by unpaired t-test.
-Figure 6H; lines 1268-1270 in the figure legend; Re-ChIP analysis shows the concurrent presence of both ERα and RARα at genomic loci of ALDH1A1 in HEC-1-AP and HEC-1-AR cells. Data are presented relative to input, showed as mean ± SD of technical triplicates and analyzed by t test.
-Figure 6I; lines 1270-1273 in the figure legend; ChIP-qPCR analysis of H3K27ac occupancy at genomic loci of ALDH1A1 in HEC-1-AR cells transfected with control siRNA, siRARA or siESR1. Data are shown as mean ± SD of technical triplicates and analyzed by unpaired t-test.
-Figure 6J; lines 1273-1276 in the figure legend; RT-qPCR validation of RARA and ALDH1A1 in HEC-1-AR and HEC-1-BR cells transfected with control siRNA or RARA siRNA. Data are shown as mean ± SD of technical triplicates and analyzed by unpaired t-test.
-Figure 6K; lines 1276-1278 in the figure legend; RT-qPCR validation of ESR1 and ALDH1A1 in HEC-1-AR and HEC-1-BR cells transfected with control siRNA or ESR1 siRNA. Data are shown as mean ± SD of technical triplicates and analyzed by unpaired t-test
-Figure 6M; lines 1281-1284 in the figure legend; ChIP qPCR analysis of H3K27ac, ERα and RARα occupancy at genomic loci of ALDH1A1 in HEC-1-AP cells treated with DMSO and RA (20 μM) for 72 hours. Data are presented relative to input, shown as mean ± SD of technical triplicates and analyzed by unpaired t-test.
-Figure 6N (up); lines 1284-1287 in the figure legend: RT-qPCR validation of ALDH1A1 in HEC-1-AP and HEC-1-BP cells treated with DMSO or RA (10 μM and 20 μM) (up). Data are shown as mean ± SD of technical triplicates and analyzed by one-way ANOVA with Dunnett's multiple comparisons test.
-Figure 7I; lines 1315-1317 in the figure legend: Determination of relative RA concentrations in PDX-EC1P and PDX-EC1R xenograft tumor tissues. Data are shown as mean ± SD of technical triplicates and analyzed by unpaired t-test.

Reviewer #2

(Remarks to the Author)
I co-reviewed this manuscript with one of the reviewers who provided the listed reports. This is part of the Nature Communications initiative to facilitate training in peer review and to provide appropriate recognition for Early Career Researchers who co-review manuscripts.

Reviewer #3

(Remarks to the Author)
The current paper addresses potential mechanisms of resistance to CDK4/6i therapy. Such small molecules are currently used in hormone receptor positive breast cancer and have therapeutic benefit. However, resistance remains an issue. Multiple mechanisms of resistance have been broadly described and most reflect non-genomic mechanisms. This paper provides evidence that increased expression of ALDH1A1 increases vitamin leading to increased retinoic acid accumulation. Critically, overexpression of ALDH1A1 was sufficient to drive resistance and it was critical for maintenance of resistance. RA accumulation led to increased RARa and ERa signaling that perpetuated ALDH1A1. This is an interesting model and much of the data was strong. However, there are significant issues that need to be addressed. The most significant of which is how SE are called from the genomic experiments. It is not described and it seems that enhanced H2K27ac is the only marker for SE. This is not fully justified and further it is unclear what or how SE were called; how much of an increase or clustering. Ultimately, while ALDH1A1 is up, it is far from clear that this reflects SE increase and further what drives this mechanism. Additional points follow.

1. How SE are called from the genomic experiments. It is not described and it seems that enhanced H2K27ac is the only marker for SE.
2. Through the paper, methods and experiments are not described with sufficient clarity to understand experimental procedures sufficiently to interpret data provided.
3. Why are the authors observing cell death with CDK4/6i? These are cytostatic drugs that trigger quiescence or ultimately senescence. This is a flaw…if death is observed, it suggests off target effects, given that in vivo death generally reflects recruitment of cytotoxic immune cells.
4. No description of proliferation assays. Is cell doubling measured? Or is this a metabolic assay used as a surrogate. If the latter, this is not valid given that C/CDK4/6 regulate cell metabolism independently of cell division.
5. The authors need to measure cell senescence with single drug and combinations.
6. In figure 4 the authors state that resistant cell "outcompete" parental cells. This experiment as described does not address competition. It simply demonstrates that resistant cells utilize more Vit A than parental.
7. How were doses of Vit A and RA? Dose response? From Literature? No description.
8. In figure 5, all conclusions are based on RNA-seq. Transcription does not necessarily reflect translation. The authors need to demonstrate that increases observed by RNA-seq are reflected at the protein level.

Reviewer #4

(Remarks to the Author)
The manuscript entitled "Targeting Super-Enhancer-1 Driven ALDH1A1-RARα/ERα Feedback Loop to Mitigate CDK4/6 Inhibitor Resistance via Suppression of Vitamin A Metabolism" by Chen et al. addresses mechanisms of resistance to CDK4/6 inhibitors (CDK4/6i), an important clinical problem. Inhibitors of CDK4/6 activity have shown promise in the clinic and palbociclib, abemaciclib, and ribociclib are FDA-approved for use in patients. However, the therapeutic promise of these agents is dampened by inevitable emergence of resistance. The authors present a compelling study in which they identify a

novel mechanism of CDK4/6i resistance involving epigenetic alterations. The study is predominantly performed in endometrial cancer (EC) models, although data from breast cancer cells are also presented. Integration of transcriptomic and chromatin data (RNA-seq and ChIP-seq data) from sensitive and resistant EC organoids and EC cell lines identified ALDH1A1 as a super enhancer-driven gene associated with CDK4/6i resistance. The authors delineate a novel positive feedback axis that promotes CDK4/6i resistance in which increased levels of ALDH1A1 accumulate in resistant cells, promoting vitamin A metabolism, accumulation of retinoic acid, interaction between RARα and ERα in the nucleus, and RARα/ERα-occupied super enhancer-driven transcriptional activation of ALDH1A1. They further determined that ALDH1A1 can be epigenetically silenced with BRD4 inhibitors to mitigate CDK4/6i resistance. Based on their findings, the authors propose that inhibition of this novel axis (e.g., ALDH1A1 inhibition) is a promising approach to re-sensitize tumors to CDK4/6i. The data are generally of good quality and supportive of the conclusions of the authors. While the study should be of interest to the broad readership of Nature Communications, the following issues should be addressed.

General:

1) In many cases (e.g., colony formation assays, Western blots), the number of biological replicates performed is not clear. While technical replicates are indicated, the number of times the experiment was carried out with similar results is not specified. This should be corrected throughout the manuscript.

2) Western blot data should be quantified, especially in experiments where changes are modest.

3) Information on the characteristics of the 16 endometrial cancer organoids generated should be provided. Were there any trends regarding the response of these organoid lines to CDK4/6i based on EC type, grade, etc?

4) Experimental details on how CDK4/6i-resistant EC cells and PDXs were generated (e.g., drug concentrations, duration of treatment at each concentration) should be included in the Materials and Methods.

5) All the experiments were performed using a single CDK4/6i inhibitor (abemaciclib) and results are expected to apply to other clinically relevant CDK4/6i. If possible, confirmation that the pathway is present in tumor cells that are resistant to another FDA-approved CDK4/6i would strengthen the study.

6) There are many language and grammatical errors throughout the manuscript that need to be addressed.

Specific Comments:

1) Fig. 3I and 3J: Near complete knockdown of BRD4 resulted in modest downregulation of ALDH1A1. Can the authors comment on other potential mediators of ALDH1A1 accumulation in CDK4/6i resistant cells?

2) Figs. 3K and 5J: A larger scale should be used on the y-axis to clarify the observed effects.

3) The data in Fig. 4M are not compelling.

4) Some of the data in Fig. 5I are not convincing (e.g., HEC-1-AR cl-Cas3). Blots of better quality should be provided and quantified.

5) The graph on the right in Fig. 7A appears to be mislabeled.

6) In Fig. 7B, there appears to be a robust effect of Abem on HEC-1-AR tumor weight. Can the authors explain this effect in resistant cells?

7) Supplemental Fig. 5C: Levels of cyclin D1 protein should be shown.

Version 1:

Reviewer comments:

Reviewer #1

(Remarks to the Author)
The authors have revised their manuscript in response to the reviewers' suggestions, and several aspects have improved. Nonetheless, some points remain that require clarification or further detail.

Response to comment 1 and 2:
The methodological description used to determine the IC50 values in Fig. 1C and the Response Fig. 1A requires some further clarification in the Methods section. Based on the graphs, we assume that PDOs were exposed to the drug concentrations indicated on the y-axis, however this should be stated somewhere. In addition, we could not find information on "MAcreGel" and Mingao Biotech.
We appreciate the inclusion of the new data on Palbociclib and Ribociclib. It would be important to clarify whether these experiments were performed in parallel with the Abemaciclib treatments. The striking similarity of the responses raises the

question whether the PDOs display a general, non-specific sensitivity or reduced survival capability rather than a selective response to the individual CDK4/6 inhibitors. It may be worth testing additional more monospecific CDK inhibitors, since this could help disentangle compound specific from general CDK related effects. Some work already exists that investigates the synergistic effects of ATRA with CDK inhibitors of different specificity, including ryuvidine and more selective CDK4 inhibitors.

Response to comment 5:
Regarding the ATRA concentrations used, we would like to note that pharmacokinetic studies in patients with APL indicate that the clinically applied doses result in peak plasma levels of approximately 1 µM ATRA. In our experience, concentrations as low as 10 nM ATRA can already influence RAR reporter assays. In the manuscript cited by the authors stating: “10–30 µM RA was used in HL60 and NB4 cells (11)”, one can see that although concentrations up to 30 µM were tested, 1 µM already caused the major effects on cell viability.
We therefore asked whether a concentration of 20 µM is still specific for ATRA mediated activation and transmitted by retinoic acid receptors or whether such a dose might induce additional, non specific effects, including increased expression of ALDH1A1.
Is a higher concentration required for RAR reporter activity in this particular cell type, and what would be the mechanistic explanation? How can peak plasma levels of 20 µM ATRA be reached in patients? How do other cell lines respond? Are the observed effects cell type specific? If so, we would suggest reflecting this in the title of the manuscript.

Response to comment 8:
It may be helpful to rename the primer sets (P1–4) to improve clarity. In addition, ALDH1A1 should be mentioned in the figure.

Reviewer #2

(Remarks to the Author)
I co-reviewed this manuscript with one of the reviewers who provided the listed reports. This is part of the Nature Communications initiative to facilitate training in peer review and to provide appropriate recognition for Early Career Researchers who co-review manuscripts.

Reviewer #3

(Remarks to the Author)
The authors have made extensive modifications to address concerns raised and in my opinion have addressed critical issues as needed.

Reviewer #4

(Remarks to the Author)
The authors have satisfactorily addressed the concerns raised by this reviewer in the original review.

Version 2:

Reviewer comments:

Reviewer #1

(Remarks to the Author)
All of our concerns have been satisfactorily addressed by the authors.

Reviewer #2

(Remarks to the Author)
I co-reviewed this manuscript with one of the reviewers who provided the listed reports. This is part of the Nature Communications initiative to facilitate training in peer review and to provide appropriate recognition for Early Career Researchers who co-review manuscripts.

Response Letter to Research Article-NCOMMS-25-43591A

KEY:

BLACK TEXT: Editor comments

BLUE TEXT: Author responses

RED TEXT: Changes made to text in manuscript

****

REVIEWER COMMENTS

Reviewer #1 (Remarks to the Author):

In this study, Chen and colleagues investigated the effects of abnormal ALDH1A1 expression on CDK4/6i resistance in hormone receptor-positive breast and endometrial cancers. The researchers demonstrate that high ALDH1A1 levels and their downstream effects contribute to CDK4/6i insensitivity.

Response to Reviewer: We appreciate the positive comments from the Reviewer. We believe that we have fully addressed all the concerns in the point-by-point responses below.

We have some comments:
1) The methodology used for the sensitivity profiling of abemaciclib against 16 PDOs from EC is unclear. How do other CDK4/6 inhibitors such as Palbociclib and Ribociclib compare? Is the response CDK4- or CDK6-specific?

Response to Reviewer: We appreciate the constructive suggestions from the Reviewer. We have amended the description of methodology used for the sensitivity profiling of CDK4/6 inhibitors in the Method section (Page 23-24): "For the cell viability assay, organoids were harvested and dissociated using TrypLE™ Express (Gibco, 12604013) for 10 min at 37 ºC. The dissociated PDOs were resuspended in ice-cold MAcreGel (Mingao Biotech) and seeded into a 96-well plate (Corning). After allowing the MAcreGel drops to solidify for 15 min at 37 ºC, PDOs were overlaid with endometrial cancer organoid medium containing the indicated doses of drugs. Five days after drug treatment, cell viability was measured using the Cell Viability ATP Assay Kit (Mingao Biotech) according to the manufacturer's instructions on a Spark microplate reader (Tecan)."

As for the sensitivity of PDOs to other CDK4/6 inhibitors, we have conducted cell viability assay using other clinically used CDK4/6 inhibitors (e.g., Palbociclib, Ribociclib) to assess the half-maximal inhibitory concentration (IC50) values of 16 PDOs (**Response Figure 1A**). The results showed that PDOs exhibit comparable sensitivity to both Palbociclib/Ribociclib and Abemaciclib, suggesting that the

sensitivity of PDOs to CDK4/6 inhibitors stems from their CDK4/6-specific on-target effect rather than a unique response to a single inhibitor. We have appended Response Figure 1A to Supplemental Figure 1 with the description (Page 6): "In addition, the response to CDK4/6 inhibition in PDOs was confirmed with other CDK4/6 inhibitors (Palbociclib and Ribociclib) (Supplementary Fig. 1A-B)."

As the Reviewer mentioned whether the response of CDK4/6i was CDK4- or CDK6-specific, we analyzed the expression levels of CDK4 and CDK6 in the EC tumors from RNA-seq data. The results showed no statistical difference in expression levels of CDK4 or CDK6 between sensitive and resistant groups to CDK4/6i (**Response Figure 1B**), indicating that the response to CDK4/6i may be independent of CDK4 or CDK6.

Response Figure 1

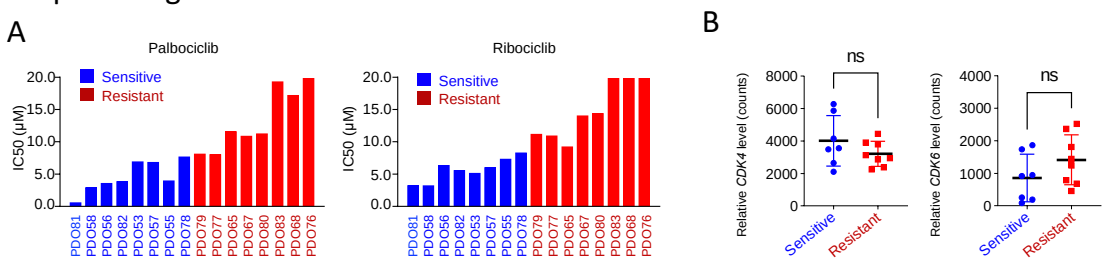

Response Figure 1. (A) Growth-inhibitory effect of 16 PDOs treated with different doses of Palbociclib and Ribociclib. The y-axis shows the IC50 values. (B) The counts of indicated genes in EC tumors from RNA-seq data.

2) What dose is considered the threshold for Abemaciclib resistance in vitro? In Supplementary Figure 2, the authors show response curves from a wide variety of endometrial cancer cells. Indicating IC50 values would increase the interpretability of the results.

Response to Reviewer: We thank the Reviewer for pointing out this issue. We defined the Abemaciclib-resistant cell lines using an IC50 cut-off value of 1.0 μM. We have updated the IC50 values of Abemaciclib for the indicated cells and amended them in the revised version as follows.

Response Figure 2

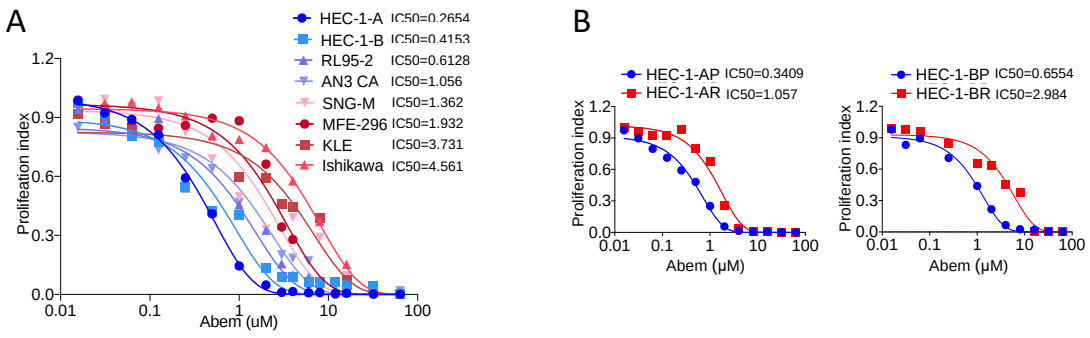

Response Figure 2. (A) EC cell lines were treated with the indicated concentrations of Abemaciclib. The number of viable cells was measured at 96 hours. Data are represented the mean of three independent replicates. The IC50 values of Abemaciclib for EC cell lines after exposure durations of 96 hours are shown. (B) Parental and resistant cells treated with the indicated concentrations of Abemaciclib. The number of viable cells was measured at 96 hours. Data are represented the mean of three independent replicates. The IC50 values of Abemaciclib for HEC-1-AP, HEC-1-AR, HEC-1-BP and HCE-A-BR after exposure durations of 96 hours are shown.

3) Quantification and replicates of analyses in Figure 3, as the effects of knockdown, overexpression of ALDH1A1 or its inhibition, and others throughout the manuscript seem to be missing. Moreover, in the manuscript, considerable amount of conclusions were drawn from visual data, such as colony formation assays and immunofluorescence / immunohistochemistry. Although they might still convey the main idea, the quality of the visuals is low, making a through revision challenging. It is essential that the manuscript includes either significantly improved visuals or clear, detailed quantitative data to support the findings. As an example, in Figure 2K, although the difference is clear, the cells in the resistance group look rather overexposed, very likely due to image quality. Additionally, immunofluorescence images should include a legend indicating the color assigned to each marker.

Response to Reviewer: We thank the Reviewer for pointing out these issues. We have quantified the intensity of all the bands in the Western Blot experiments using ImageJ/Fiji software and labeled the normalized relative gray values in the updated version of the manuscript. In addition, we have performed statistical analysis of all colony formation assays and their corresponding replicate experiments using ImageJ/Fiji software. We have also updated the images to high-resolution to correct those with suboptimal exposure in all image data (**Response Figure 3**). Furthermore, we have added color legends to immunofluorescence images to indicate the corresponding colors for each marker (**Response Figure 4**). The updated images and figures are provided in **Response Figure 3,** and we have amended the previous Figure 3 with this Response Figure 3 in our manuscript.

In Method section (Page 22): "The colonies were quantified using ImageJ/Fiji software (https://fiji.sc/)."

In Method section (Page 24): "The blots were quantified using ImageJ/Fiji software (https://fiji.sc/)."

In Figure Legend section (Page 41): "Representative immunofluorescence (IF) images of HEC-1-AP, HEC-1-AR, HEC-1-BP and HEC-1-BR cells stained with ALDH1A1, scale bar = 10 μm, blue color shows DAPI signal, green color shows ALDH1A1 signal. (left). The intensity of ALDH1A1 in parental and resistant cells were quantified and analyzed by t test. ***$p < 0.001$. (right)."

Response Figure 3

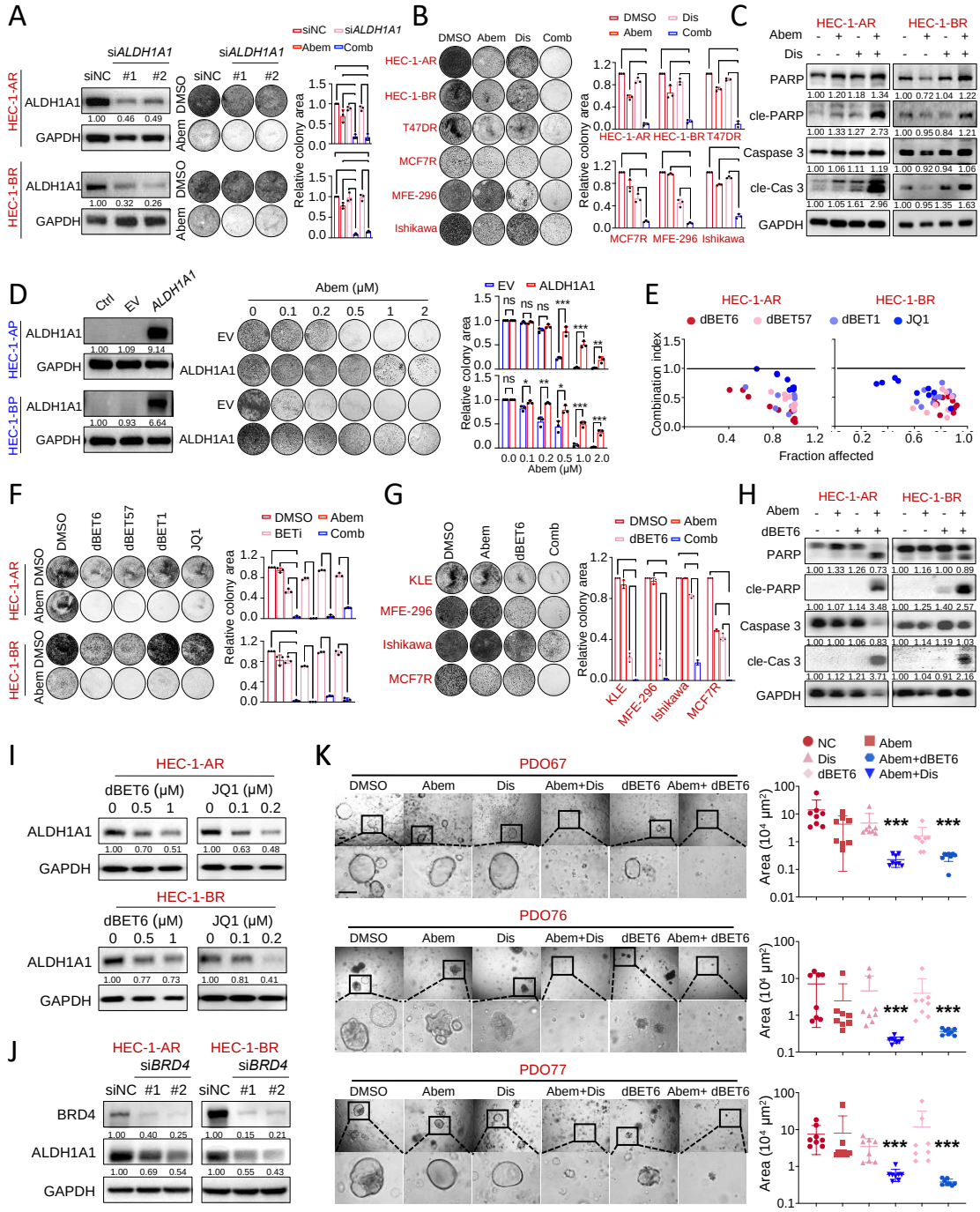

Response Figure 3. (A) Immunoblot analysis of ALDH1A1 in HEC-1-AR and HEC-1-BR cells transfected with control siRNA or ALDH1A1 siRNA. Shown are representative blots from three independent experiments. (left). Representative images and quantification of colony formation assay in cells treated with siNC, siALDH1A1, Abemaciclib (0.5 μM), or combination. Data are shown as mean ± SD of three independent experiments and analyzed by One-way ANOVA with Dunnett's multiple comparisons test. ***$p < 0.001$. (right). (B) Representative images and quantification of colony formation assay in cells treated with DMSO, Abemaciclib (Abem) (0.5 μM), Disulfiram (Dis), or combination in the indicated cells. Data are shown as mean ± SD of three independent experiments and analyzed by One-way ANOVA with Dunnett's

multiple comparisons test. ***$p < 0.001$. (C) Immunoblot analysis of PARP, cleaved-PARP, Caspase 3 and cleaved-Caspase 3 in HEC-1-AR and HEC-1-BR cells treated with DMSO, Abemaciclib (0.5 μM), Disulfiram (1 μM for HEC-1-AR and 2 μM for HEC-1-BR), or combination for 72 hours. Shown are representative blots from three independent experiments. (D) Immunoblot analysis of ALDH1A1 expression in HEC-1-AP/HEC-1-BP cells (control), overexpressing empty vector (EV) or ALDH1A1. Shown are representative blots from three independent experiments. (left). Representative images and quantification of colony formation assay in HEC-1-AP/HEC-1-BP cells overexpressing empty vector (EV) or ALDH1A1, which were treated with Abemaciclib (0.5 μM). Data are shown as mean ± SD of three independent experiments and analyzed by unpaired t-test. ns, not significant, *$p < 0.05$, **$p < 0.01$, ***$p < 0.001$. (right). (E) CI analysis of Abemaciclib and BRD4 inhibitors in resistant cell lines. Data are represented the mean of 3 biological replicates. CI greater than 1 is defined as antagonism; CI less than 1 is defined as synergy. (F) Representative images and quantification of colony formation assay in HEC-1-AR and HEC-1-BR cells treated with DMSO, Abemaciclib (0.5 μM), dBET6 (0.5 μM for HEC-1-AR and 2 μM for HEC-1-BR), dBET57 (2 μM for HEC-1-AR and 10 μM for HEC-1-BR), dBET1 (2 μM for HEC-1-AR and 5 μM for HEC-1-BR), JQ1 (0.2 μM), or combination. Data are shown as mean ± SD of three independent experiments and analyzed by One-way ANOVA with Dunnett's multiple comparisons test. ***$p < 0.001$. (G) Representative images and quantification of colony formation assay in KLE, MFE-296 and Ishikawa cells treated with DMSO, Abemaciclib (0.5 μM), dBET6 (0.25 μM for KLE, 0.5 μM for MFE-296 and Ishikawa, 0.1 μM for MCF7R), or combination. Data are shown as mean ± SD of three independent experiments and analyzed by One-way ANOVA with Dunnett's multiple comparisons test. ***$p < 0.001$. (H) Immunoblot analysis of PARP, cleaved-PARP, Caspase 3 and cleaved-Caspase 3 in HEC-1-AR and HEC-1-BR cells treated with DMSO, Abemaciclib (0.5 μM), dBET6 (0.5 μM for HEC-1-AR and 2 μM for HEC-1-BR), or combination for 72 hours. Shown are representative blots from three independent experiments. (I) Immunoblot analysis of ALDH1A1 expression in HEC-1-AR and HEC-1-BR cells treated with BRD4 inhibitors (dBET6 and JQ1) for 72 hours. Shown are representative blots from three independent experiments. (J) Immunoblot analysis of ALDH1A1 expression in HEC-1-AR and HEC-1-BR cells transfected with control siRNA or BRD4 siRNA for 72 hours. Shown are representative blots from three independent experiments. (K) Representative images of PDO67, PDO76 and PDO77 treated with DMSO, Abemaciclib (1 μM), Dis (2 μM), dBET6 (2 μM), or combination after 10 days culture. The experiment was performed in three biological replicates. Scale bar = 200 μm. (left). The matching scatter diagram shows surface area of organoids, and one dot represents one organoid. Data are shown as mean ± SD and analyzed by Kruskal-Wallis with Dunn's multiple comparisons test. ***$p < 0.001$. (right). Source data of (A), (C-F), (H-K) are provided in Source Data file.

Response Figure 4

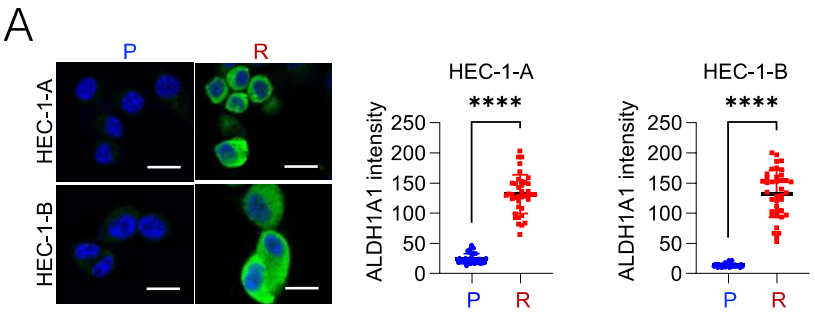

Response Figure 4. (A) Representative immunofluorescence (IF) images of HEC-1-AP, HEC-1-AR, HEC-1-BP and HEC-1-BR cells stained with ALDH1A1, scale bar = 10 μm, blue color shows DAPI signal, green color shows ALDH1A1 signal. (left). The intensity of ALDH1A1 in parental and resistant cells were quantified and analyzed by t test. ***$p < 0.001$. (right).

4) The ChIP-seq data and others don't seem to be available for review. Has it been uploaded to a repository? No quality metrics seem to be provided. What where the controls in these experiments?

Response to Reviewer: We thank the Reviewer for pointing out these issues. ChIP-seq data generated in this study have been deposited in the Genome Sequence Archive in the National Genomics Data Center, China National Center for Bioinformation/Beijing Institute of Genomics, Chinese Academy of Sciences (GSA-Human: HRA008718). Following online publication of this study, the data will be accessible via https://ngdc.cncb.ac.cn/gsa-human, which has been described in the Method section. During the peer review stage, we provided a data access link in the nature portfolio Reporting Summary (https://ngdc.cncb.ac.cn/gsa-human/s/udT1vJ7Y).

For the quality control (QC) of ChIP-seq data in our study, we ensured sufficient sequencing depth (≥20 million uniquely mapped reads per sample) to capture specific binding events. Samples were excluded with low mapping rates (<80%). Reads with duplicates were removed by rmdup for the subsequent analysis. Significant peaks were called using MACS2 ($p < 0.05$). For the control groups of each experiment, we included critical input DNA controls: genomic DNA from the same cell/tissue sample (without ChIP enrichment) was sequenced to distinguish specific protein-DNA binding from background genomic noise, and we used it to normalize peak signals in downstream analysis.

We have provided detailed information for the quality control and analysis process in the Method section (Page 28):

"Cells were cross-linked with 1% formaldehyde and quenched with 0.125 M glycine. The cross-linked cells were lysed in the lysis buffer (50 mM Tris-HCl [pH 8.0], 10 mM EDTA, 1% SDS) and sonicated on ice using a Bioruptor (Glen Mills, Qsonica Q700, USA). The lysates were precleared with protein G Dynabeads (Invitrogen), and 5% precleared lysates were taken to elute, reverse cross-linked, and purify for Input-DNA.

Immunoprecipitated with protein G Dynabeads (Invitrogen) and incubated with the antibody-beads complex overnight at 4°C. Immunoprecipitations were eluted, reverse cross-linked, and purified for ChIP-DNA."

And in the Method section (Page 30):

"For ChIP-seq analyses, the clean data were generated from fastp and mapped against the human reference genome (GRCh38, hg38) using Bowtie2 (version 2.3.2) under default settings.(1) Samples were excluded with low sequencing depth (< 20 million reads) and mapping rates (<80%). Reads with duplicates were removed by rmdup for the subsequent analysis. The alignments were sorted and indexed using samtools (version 1.14).(2) Peaks were identified using MACS2 (version 2.1; $p < 0.05$) (3) and annotated with ChIPseeker (version 1.14.2). Super enhancer regions were obtained using ROSE with H3K27ac peaks.(4) DNA motif analysis was performed using Homer (homer.salk.edu) with default settings.(5) Bigwig files produced by deepTools were visualized in Integrative Genomics Viewer (version 2.4.19).(6, 7) For each ChIP-seq experiment, we included critical input DNA controls: genomic DNA from the same cell/tissue sample (without ChIP enrichment) was sequenced to distinguish specific protein-DNA binding from background genomic noise, and we used it to normalize peak signals in downstream analysis."

5) In the experiments shown in Figure 4A and Figure 6M, the authors indicate that they treat the cells with 20 μM ATRA. In our experience this is way over the relevant in vitro therapeutic dose, which is conventionally between 0.01-1 μM. This is also valid for Vitamin A treatments - the authors should test if the effects of RA and Vitamin A are dose-dependent, in order to ensure that very high doses are not skewing the responses away from what is physiologically and therapeutically relevant.

Response to Reviewer: We thank the Reviewer for pointing out this issue. To investigate whether the effects of RA and VitA are dose-dependent, we performed experiments with concentration gradient ranging from 0.1 to 50 μM of RA/VitA to treat the HEC-1-A and HEC-1-B cells. As the drug concentration increased, the expression of *ALDH1A1* also increased significantly in a dose-dependent manner (**Response Figure 5A-B**). We treated the cells with Abemaciclib in combination with increased concentrations of RA or vitA. The results showed that the effects of RA and vitA in mediating the Abemaciclib resistance became more pronounced as their concentrations increased (**Response Figure 5C-D**). In addition, the cell viability was not impaired by the increasing dosages of RA or vitA (**Response Figure 5E-F**). Therefore, we used 20 μM RA and 10 μM VitA for further experiments to obtain the optimal results.

Actually, the concentration ranges of RA and VitA in cellular experiments vary depending on cell types, experimental purposes, and mechanisms of action. For example, 20 μM RA was used in MDA-MB-231 cells, where cell viability was not affected.(8) In addition, 2 μM RA was used in transfected HEK-293T cells for luciferase reporter assay (9), 10 μM RA was used in human neuroblastoma SH-SY5Y cells (10), and 10-30 μM RA was used in HL60 and NB4 cells.(11) As for vitA concentrations, Cabezas-Wallscheid N et al. treated hematopoietic stem/progenitor

cells with 10 μM VitA. (12) Colucci M et al. treated RWPE-1 and 22RV1 cells with 10 μM VitA. (13) These reports indicated that a wide range of RA/VitA doses were used in different studies.

We have amended the description in the Result section (Page 11). "Moreover, the effects of RA and vitA in mediating the Abemaciclib resistance became more pronounced as their concentrations increased (Supplementary Fig. 4E-F)."

Response Figure 5

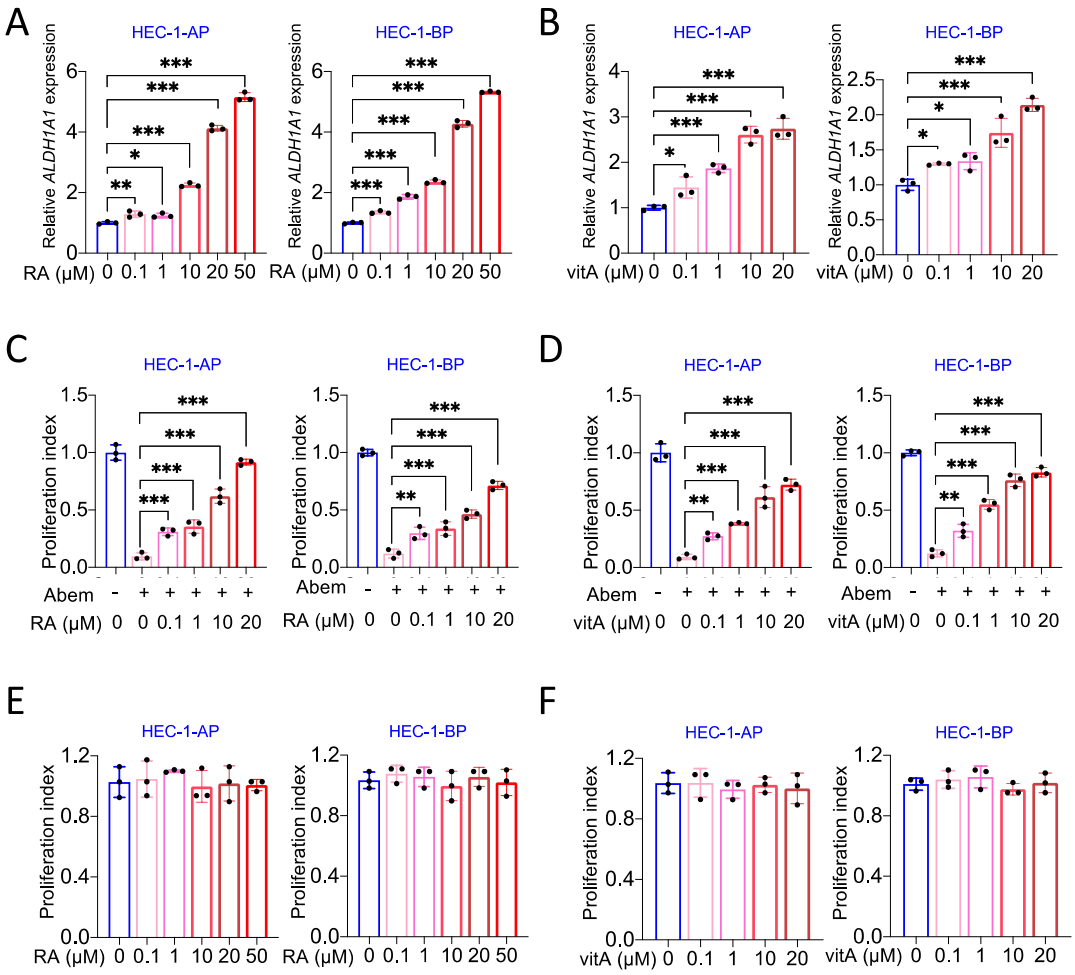

Response Figure 5. (A-B) RT-qPCR validation of ALDH1A1 in HEC-1-AP and HEC-1-BP cells treated with DMSO, RA (0.1 μM, 1 μM, 10μM, 20 μM and 50 μM) or vitA (0.1 μM, 1 μM, 10 μM and 20 μM). Data are shown as mean ± SD of and analyzed by one-way ANOVA with Dunnett's multiple comparisons test. (C-D) HEC-1-AP and HEC-1-BP cells treated with combinations of RA (0 μM, 0.1 μM, 1 μM, 10 μM and 20 μM) and Abemaciclib (0.5 μM), or combinations of vitA (0 μM, 0.1 μM, 1 μM, 10 μM and 20 μM) and Abemaciclib (0.5 μM). The number of viable cells is measured at 96 hours. Data are shown as mean ± SD and analyzed by one-way ANOVA with Dunnett's multiple comparisons test. (E-F) HEC-1-AP and HEC-1-BP cells treated with RA (0 μM, 0.1 μM, 1 μM, 10 μM and 20 μM) and the number of viable cells is measured at 96 hours. Data are shown as mean ± SD. *$p < 0.5$, **$p < 0.01$, ***$p < 0.001$.

6) In Figure 2J, what do P1, 2, 3, and 4 correspond to? In the legend it was stated that the data was shown as mean ± SD of technical triplicates. If they are biological replicates, it would be more sensible to show the cumulative data as n=4 and perform statistics. Moreover, the graph type that was chosen is not suitable for a t-test.
In general, the number of biological replicates seems not to be indicated in all of the experiments, so the authors should provide this information.

Response to Reviewer: We thank the advises from the Reviewer. P1–P4 represent the ChIP primers across the SE regions of *ALDH1A1*, which was shown in the Supplemental Figure 2I. We have amended the description in the Result section (Page 8-9): "Next, we designed ChIP primers (P1-P4) across the SE regions of *ALDH1A1* (Supplementary Fig. 2J), performed ChIP-qPCR analysis and found significant enrichment of H3K27ac binding at the ALDH1A1 locus in resistant cells (Fig. 2J)."

We apologized for the mistake in describing "technical triplicates" in the original legend. Actually, the experiments in Figure 2J were performed in three independent biological replicates, we performed technical triplicates to ensure detection accuracy during each independent biological replicate. After verifying the consistency of technical triplicates, we calculated the mean value of each independent biological experiment's technical triplicates as the final data point for that sample. We have corrected the descriptions in the figure legend in the revised version of the manuscript. The updated figures are shown as follows (**Response Figure 6A**) and the repetitive data were shown in Source Data.

In Figure 2J, the analysis was specifically focused on comparing the enrichment levels of H3K27ac binding at the four gene loci P1, P2, P3, and P4 of *ALDH1A1* between two independent groups: parental and resistant cells. The use of an independent samples t-test is appropriate.

All experiments in the study were performed at least three times from biological replicates or independent experimental replicates. And we have annotated the number of independent samples/experiments for all experiments in the updated versions.

Response Figure 6

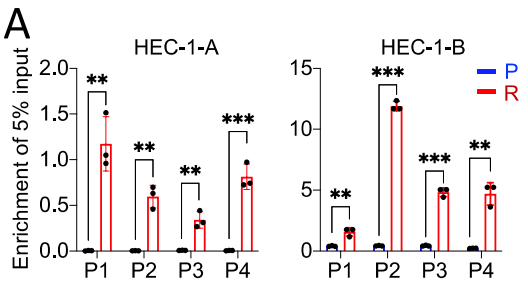

Response Figure 6. (A) ChIP-qPCR analysis of H3K27ac occupancy at genomic loci of *ALDH1A1* (P1-4) in parental (P) and resistant (R) cells. Data are presented relative

to input, shown as mean ± SD of three independent experiments and analyzed by unpaired t-test. $**p < 0.01$, $***p < 0.001$.

7) Throughout the manuscript, some data were shown as mean ± SD, while some were shown as mean ± SEM (although authors only stated it as ± SEM, which needs additional correction). The data presentation must follow a uniform format to ensure clarity and consistency across the manuscript.

Response to Reviewer: We thank the Reviewer for the advises. All the data previously shown as mean ± SEM were re-analyzed and were presented as mean ± SD in the updated version.

8) The authors established 4 Abemaciclib resistant cell models with HEC-1-A, HEC-1-B, MCF7 and T47D cells through chronic exposure. Figure 2A indicates that they used increasing doses of Abemaciclib, while DMSO seems to be constant. In our experience DMSO itself might have substantial effect on the cells. Was DMSO amount also increased in parallel? The authors should describe the establishment of their acquired resistance models in more detail.

Response to Reviewer: We thank the Reviewer for pointing out this issue. The DMSO amount was increased in parallel during the establishment of drug-resistant cells. Since Abemaciclib was dissolved in DMSO, each time the concentration of Abemaciclib was increased, the DMSO level was adjusted synchronously in both parental and resistant cells to ensure consistency between the two groups. Given that DMSO itself exhibits certain cellular toxicity, its final concentration in the cell culture medium was maintained at ≤ 0.1% according to previous studies.(14) Consequently, although the DMSO concentration may increase slightly with rising Abemaciclib concentrations, this increase is essentially negligible.

We have amended the description of methodology about constructing acquired resistance models in the Method section (Page 22-23):

"**Establishment of cell lines with acquired resistance to Abemaciclib**

Cells were grown with progressively increasing concentrations of Abemaciclib. Subconfluent cells were treated with Abemaciclib at IC50 doses (based on 96-hour cytotoxicity assays) for two 3-day periods, and surviving cells were maintained for another 4 days. The process was repeated once, and the remaining cells were cultured in the presence of drug for 3 additional passages. Resistant cells were maintained in the presence of Abemaciclib, and the same passage parental cells were treated with the same dose of DMSO."

9) The authors had 8 EC cells lines at the hand, why did they choose to move forward with HEC-1-A and HEC-1-B cells, since HEC-1-B is the substrain of HEC-1-A cells and therefore very similar? Wouldn't a more distinct cell model be preferable?

Response to Reviewer: We thank the Reviewer for pointing out this issue. HEC-1-A, HEC-1-B, RL95-2, KLE, Ishikawa, MFE-296, AN3 CA, and SNG-M cells are commonly used endometrial cancer cell lines in multiple studies. Among these strains, we identified HEC-1-A and HEC-1-B cells as the most sensitive cells to CDK4/6i in the IC50 profiling (**Response Figure 7A**). Consequently, these two cell lines were utilized to establish acquired-resistance models. Although HEC-1-B is a substrain of HEC-1-A cells, significant differences exist between them in genomic and protein expression characteristics, and both are extensively used in various studies.(15-17) More importantly, in this study, our findings were further validated in multiple additional models, including breast cancer cell lines T47D and MCF7 (Fig. 2I, Fig. 2L, Fig. 3B, Fig. 5H), CDK4/6i resistant cell lines T47DR, MCF7R, MFE-296 and Ishikawa (Fig. 3B, Fig. 3G, Supplementary Fig. 5B), three cases of PDOs (Fig. 3K, Fig 5J), two cases of PDX models (Fig. 7) and clinical samples. These data collectively support the reliability of the findings and conclusions presented herein.

Response Figure 7

A

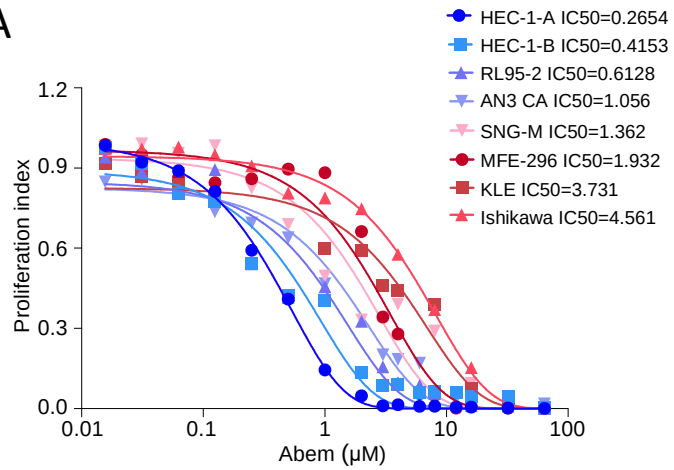

Response Figure 7. (A) EC cell lines were treated with the indicated concentrations of Abemaciclib. The number of viable cells was measured at 96 hours. Data are represented the mean of three independent replicates. The IC50 values of Abemaciclib for EC cell lines after exposure durations of 96 hours are shown.

10) In Figure 1J, the authors show enrichment of epithelial mesenchymal transition (EMT), KRAS and estrogen response signaling in resistant tumors, not surprisingly so, considering KRAS is known to be frequently mutated in Type I endometrial EC, which represents 87.50% of the cohort of the study. Can authors provide information regarding KRAS status of their patient cohort? Could KRAS activating mutations already be an indication of resistance? The same question also stands for the dataset they use for T47D palbociclib resistance model - KRAS is also highly expressed in T47D. Could the palbociclib treatment select the cells with strong KRAS signaling and have increased EMT features? Notably, given that these pathways appear critical to their resistance models, how might the authors relate this to their current findings? Does

KRAS activation favor higher ALDH1A1 activity as well? Additionally, as EMT was shown to be a key feature of Abemaciclib resistance, did authors observe any change in the EMT features in their ALDH1A1 overexpression / silencing models? These points should be more clearly integrated into the manuscript to strengthen the overall narrative of the work.

Response to Reviewer: We thank the Reviewer for pointing out these issues. To determine the mutation status of *KRAS* in our cohort, we have performed Sanger sequencing to detect mutations in *KRAS* in tumor tissues. Among the 16 EC samples, 4 cases (25%) of them contained *KRAS* mutations, which was similar to previous studies that about 20% mutation rates of KRAS were present in EC.(18, 19) In addition, the same frequency of *KRAS* mutations was found in sensitive group (2/8, 25%) and resistant group (2/8, 25%) (**Response Figure 8A**), which was in line with the study in breast cancer patients that the *KRAS* mutation status was not relative to the response of CDK4/6i. (20) Based on these findings, *KRAS* activating mutation served as an indication of CDK4/6i resistance needs to be further investigated.

To clarify whether CDK4/6i treatment could select the tumor cells with strong KRAS signaling and increase EMT features, we detected expression of multiple key markers including p-ERK, p-MEK, E-cadherin and Vimentin in parental and resistant cells. The results showed that the resistant cells have stronger KRAS and EMT signaling (**Response Figure 8B**), which were consistent with the findings from RNA-seq (Fig. 1I-K).

To determine whether KRAS activation favors higher ALDH1A1 activity, we treated tumor cells with KRAS inhibitor (BI-2865) and found no significant changes of ALDH1A1 expression (**Response Figure 8C**). In addition, we found that knockdown of ALDH1A1 suppress expression of p-ERK, p-MEK and EMT features, while overexpression of ALDH1A1 reversed the effect, which were in line with previous reports (**Response Figure 8D**).(21-23) These results indicated that the resistance to CDK4/6i induced by RARα-ALDH1A1 axis might partially occur through the regulation downstream effectors in KRAS and EMT signaling pathways. Thus, further investigation would be valuable to clarify regulatory network between ALDH1A1 and KRAS/EMT signaling.

We appreciate the Review's comments and agree that these points are important and can strengthen the overall narrative of the work. We have revised the description in the Result section and updated the Supplementary Figures as follows:

In Result section (Page 7): "Among these tumors, *KRAS* mutations were detected in 25% (4/16) of tumors, which showed the same frequency of *KRAS* mutations in the sensitive groups (2/8, 25%) and the resistant groups (2/8, 25%) (Supplementary Table. S2). These data are in line with the study in breast cancer patients that the *KRAS* mutation status was not relative to the response of CDK4/6i.(20)"

In Result section (Page 14): "Consistent with the findings in RNA-seq (Fig. 1), CDK4/6i-resistant cells exhibit strong KRAS signaling and EMT features (Supplementary Fig. 5L). Moreover, knockdown of ALDH1A1 suppressed the expression of p-ERK, p-MEK and EMT markers, while overexpression of ALDH1A1

upregulated their expression (Supplementary Fig. 5M). These results indicated that resistance to CDK4/6i induced by RARα-ALDH1A1 axis might partially occur through the regulation of downstream effectors in KRAS and EMT signaling pathways."

Response Figure 8

A

KRAS Mutation types in EC patients.

Patient	Response	Mutation type
UCEC1153	Sensitive	Wild-type
UCEC1155	Sensitive	*KRAS-G12C*
UCEC1156	Sensitive	Wild-type
UCEC1157	Sensitive	Wild-type
UCEC1158	Sensitive	Wild-type
UCEC1178	Sensitive	*KRAS-G12D*
UCEC1181	Sensitive	Wild-type
UCEC1182	Sensitive	Wild-type
UCEC1165	Resistant	Wild-type
UCEC1167	Resistant	*KRAS*-G12V
UCEC1168	Resistant	Wild-type
UCEC1176	Resistant	Wild-type
UCEC1177	Resistant	*KRAS-G12A*
UCEC1179	Resistant	Wild-type
UCEC1180	Resistant	Wild-type
UCEC1183	Resistant	Wild-type

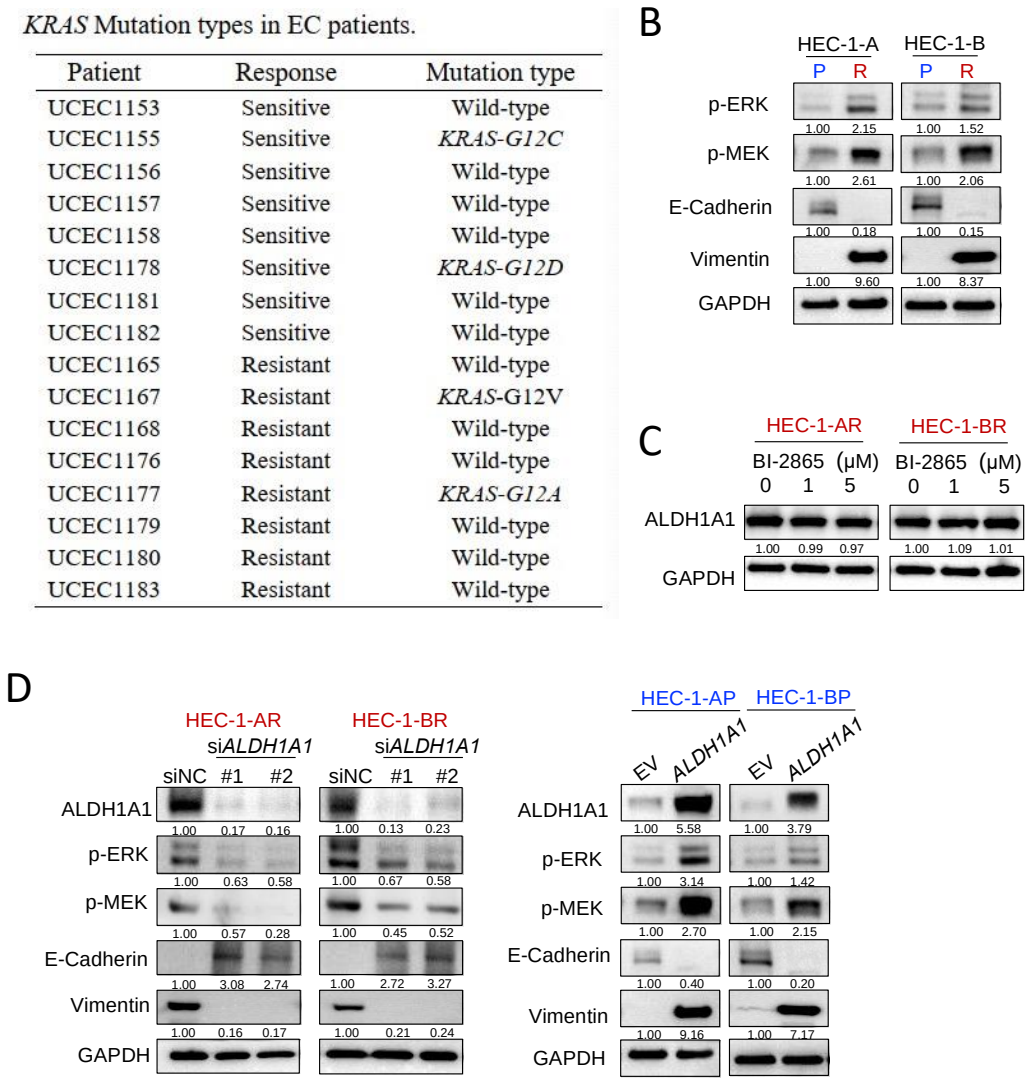

Response Figure 8. (A) *KRAS* mutation types in EC patients. (B) Immunoblot analysis of p-ERK, p-MEK, E-cadherin and Vimentin in indicated cells. (C) Immunoblot analysis of p-ERK, p-MEK, E-cadherin and Vimentin in HEC-1-AR and HEC-1-BR cells transfected with control siRNA or *ALDH1A1* siRNA (left), or in HEC-1-AP and HEC-1-BP cells overexpressing empty vector (EV) or *ALDH1A1* (right).

11) In lines 144-146, authors state that their histological analyses showed morphological similarities between PDOs and their corresponding primary EC tumors. However, PDOs exhibited great distinction in sensitivity to CDK4/6i Abemaciclib. In its current form, the sentence implies that authors tested Abemaciclib sensitivity of tumors before the PDOs were formed and there is a difference after PDO formation. If

this was done, the authors should show the data and discuss the potential mechanisms. If not, the sentence should be revised.

Response to Reviewer: We appreciate the Reviewer for pointing out the misleading implication in the original statement. We only tested the sensitivity of PDOs to Abemaciclib after their establishment in our study. We have revised the sentence in the updated version as follows.

In Result section (Page 6) "After the establishment of the PDOs, we performed histological analyses and showed that the morphology of PDOs was similar to that of their corresponding primary EC tumors (Fig. 1B). We subsequently profiled the sensitivity of 16 PDOs to Abemaciclib. However, these PDOs exhibited great distinction in sensitivity to CDK4/6i Abemaciclib (Fig. 1B-C)."

12) For experiments with viral transduction, such as in Figure 3D, comparisons focus on control groups, but the relationship between empty vector controls and parental cells is not addressed.

Response to Reviewer: We thank the Reviewer for pointing out this issue. To elucidate the relationship between the empty vector control group and parental cells, we assessed the sensitivity of parental cells, as well as parental cells overexpressing EV or ALDH1A1, to Abemaciclib via colony formation assays in both HEC-1-AP and HEC-1-BP cells. The results showed no significant differences in either ALDH1A1 expression or sensitivity to Abemaciclib between parental cells and cells overexpressing EV (**Response Figure 9A-C**).

A number of comparable studies in the literature omitted blank controls in their experimental design.(24-26) However, in the interest of experimental rigor and reliability, we fully agree with the reviewer's recommendation that blank controls are of great importance, and we will ensure greater attention to this critical experimental detail in future studies.

Response Figure 9

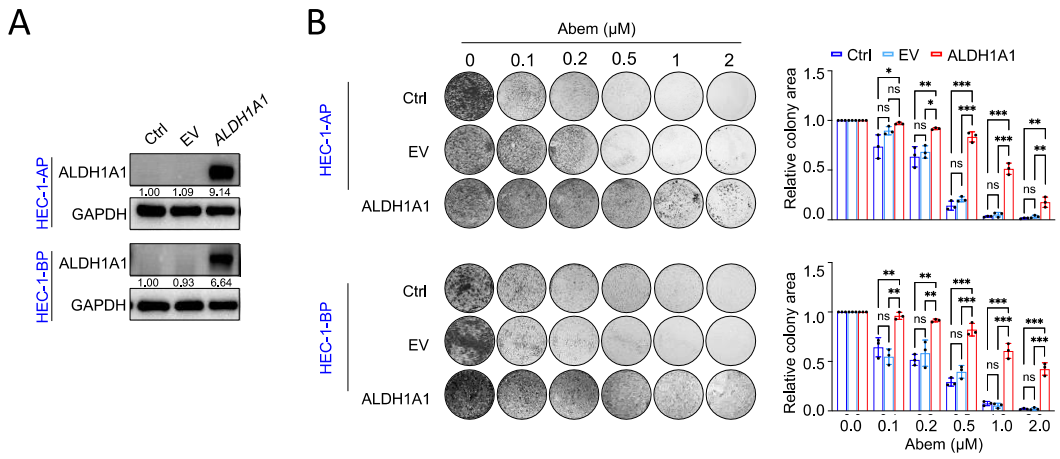

Response Figure 9. (A) Immunoblot analysis of ALDH1A1 expression in HEC-1-AP/HEC-1-BP cells (control), overexpressing empty vector (EV) or *ALDH1A1*. Shown

are representative blots from three independent experiments. (B-C) Representative images (B) and quantification (C) of colony formation assay in HEC-1-AP/HEC-1-BP cells (control), overexpressing empty vector (EV) or ALDH1A1, which were treated with Abemaciclib (0.5 μM). Data are shown as mean ± SD of three independent experiments and analyzed by One-way ANOVA with Dunn's multiple comparisons test. ns, not significant, *$p < 0.05$, **$p < 0.01$, ***$p < 0.001$.

13) In Figure 4H, the scatter diagrams show the IC50 of Palbociclib in GDSC database between high and low activation of vitA metabolic, RA signaling, RA metabolic and RA nuclear binding. This is particularly interesting, considering CDK4/6i such as palbociclib are considered candidate drugs to be used in combination for differentiation therapy in cancers such as acute myeloid leukemia and neuroblastoma (PMID: 37734383, PMID: 38507743). For the comprehensiveness of the study, it would be beneficial for the authors to address this discrepancy in the discussion.

Response to Reviewer: We thank the Reviewer for the insightful comment regarding the discrepancy of CDK4/6i and RA in acute myeloid leukemia (AML)/neuroblastoma versus our study. This discrepancy reflects the strict cancer type-specificity of CDK4/6i-RA/RARα interactions. In AML/neuroblastoma, the malignant progression of tumors relies on differentiation arrest. RA exerts its core function by promoting cellular maturation via RARα and its co-activators, including differentiation-related transcription factors, and the downstream effectors.(27-29) In this context, RARα functions as an 'initiator of the differentiation program', while CDK4/6 inhibitors suppress cell cycle progression in undifferentiated cells, thus exerting synergistic antitumor effects. However, in our models (ERα+ tumors), we found that the resistance to CDK4/6i depends on the activation of RARα/ERα signaling and the downstream ALDH1A1. The elevated RA enhances nuclear RARα-ERα interaction, promoting RARα/ERα occupancy at super-enhancers that drive ALDH1A1 transcriptional activation, leading to the CDK4/6i resistance.

We have cited these publications and discussed the discrepancies between these findings and our results in the Discussion section as follows (Page 18-19): "However, other studies have shown that CDK4/6i could promote leukemia or neuroblastoma differentiation and enhance the anti-tumor effect of RA. These studies suggested a controversial role of combination use of RA with CDK4/6i.(30, 31) Intriguingly, Palbociclib was shown as a therapeutic approach to enhance the differentiation efficacy in neuroblastoma, and it could be used in combination with retinoic acid.(30) Hu and colleagues found that CDK4/6 inhibitors synergize with ATRA to promote leukemia cell differentiation and attenuate AML cell expansion *in vivo*.(31) This discrepancy reflects the strict cancer type-specificity of CDK4/6i-RA/RARα interactions. In AML/neuroblastoma, the malignant progression of tumors relies on differentiation arrest. RA exerts its core function by promoting cellular maturation via RARα and its co-activators including differentiation-related transcription factors, and the downstream effectors.(27-29) In this context, RARα may function as an "initiator of the differentiation program", while CDK4/6 inhibitors may suppress cell cycle progression

in undifferentiated cells, thus exerting synergistic antitumor effects. However, in our models (ERα+ tumors), we found that the elevated RA potentiated the interaction between RARα and ERα in the nucleus and facilitated RARα/ERα-occupied SE-driven transcriptional activation of *ALDH1A1*, establishing a positive feedback loop that promotes CDK4/6i resistance. These studies suggest a different function of RA in CDK4/6i response in different cancer types."

14) In the study, after conducting extensive experiments, the authors identified the BRD4 inhibitor dBET6 as the most potent Abemaciclib sensitizer. While the data leading to this conclusion is solid, BET inhibitors were previously shown target ALDH1A1 super-enhancer in a 2016 work by Yokoyama & Zhu et al. (PMID: 27803105), which authors actually referenced in line 205 (Reference number 35), only to state that ALDH1A1 was a gene that was previously reported to be associated with chemoresistance. Although the two works focus on different cancer types, there are methods and conclusions that seem parallel; this should be addressed and discussed accordingly.

Response to Reviewer: We thank the Reviewer for pointing out this issue. We have discussed the related study in the updated version (Page 19): "Here, we demonstrated that ALDH1A1 is a SE-driven gene up-regulated in CDK4/6i resistance, and epigenetic suppression of ALDH1A1 with BRD4 inhibitors synergistically inhibited cell proliferation and induced cell apoptosis, ultimately overcoming the resistance to CDK4/6i. These observations were consistent with a previous study showing that BET inhibitors target the *ALDH1A1* SE and enhance the anti-tumor effect of cisplatin in ovarian cancer cells (32), suggesting that targeting SE-driven *ALDH1A1* expression could enhance the sensitivity of both chemotherapy and targeted therapy."

15) In Line 338: "Additionally, functional studies showed that genetic deletion of RARα
339 with siRNAs..." Deletion is not the correct term for siRNA.

Response to Reviewer: We thank the kind advice from the Reviewer. We have amended the description in the Results section (page 13) as follows.
"Additionally, functional studies showed that knockdown of RARα with siRNAs or pharmacological inhibition of RAR signaling with inhibitors (AGN and AR7) could overcome resistance to Abemaciclib (Fig. 5G-H and Supplementary Fig. 5C-D)."

16) In the study, substantial portion of experimental results were reported as technical replicates and yet, authors performed statistics and made certain conclusions. Since authors also showed in some the data (such as in Figure 3E) where they actually had three biological replicates, the term "technical replicates" implies that some of the experiments were performed only once, with technical replicates. The authors should either reach the number of enough biological replicates before performing statistics or correct the manuscript if it is a typographical error.

The list of experiments where only technical replicates were shown;

-Figure 2I; lines 1148-1150 in the legend: "RT-qPCR validation of ALDH1A1 in parental and resistant cells. Data are shown as mean ± SD of technical triplicates and analyzed by unpaired t-test"

-Figure 2J; lines 1152-1152 in the legend: Data are presented relative to input, shown as mean ± SD of technical triplicates and analyzed by unpaired t-test.

-Figure 3K; lines 1188-1192 in the legend: Representative images of PDO67, PDO76 and PDO77 treated with DMSO, Abemaciclib (1 μM), Dis (2 μM), dBET6 (2 μM), or combination after 10 days culture. Scale bar = 200 μm (left). The matching scatter diagram shows data as mean ± SD of technical triplicates, ***$p < 0.001$, one-way ANOVA with Dunnett's multiple comparisons test (right).

-Figure 4B: lines 1196-1199 in the legend: Determination of relative RA concentrations between parental cells (HEC-1-AP and HEC-1-BP) and resistant cells (HEC-1-AR and HEC-1-BR). Data are shown as mean ± SD of technical triplicates and analyzed by unpaired t-test.

-Figure 4C: lines 1199-1202 in the figure legend: Determination of relative vitA concentrations in cell culture medium at the indicated time points. Data are shown as mean ± SD of technical triplicates and analyzed by two-way ANOVA with Dunnett's multiple comparisons test, ***$p < 0.001$.

-Figure 4G; lines 1208-1212 in the figure legend: Resistant cells are treated with the indicated concentrations of Abemaciclib in B-27 supplement medium, vitA-deficient B-27 supplement medium or vitA-deficient B-27 supplement medium with vitA (10 μM). The number of viable cells is measured at 96 hours. Data are shown as mean ± SD of technical triplicates and analyzed by two-way ANOVA with Dunnett's multiple comparisons test, ***$p < 0.001$.

-Figure 4J; lines 1216-1218 in the figure legend: Relative ALDH enzyme activity between parental cells (HEC-1-AP and HEC-1-BP) and resistant cells (HEC-1-AR and HEC-1-BR). Data are shown as mean ± SD of technical triplicates and analyzed by unpaired t-test.

-Figure 4L; lines 1219-1221 in the figure legend: Relative ALDH enzyme activity of indicated cells. Data are shown as mean ± SD of technical triplicates and analyzed by One-way ANOVA with Dunnett's multiple comparisons test.

-Figure 4N; lines 1223-1225 in the figure legend: Determination of relative RA concentrations in indicated cells. Data are shown as mean ± SD of technical triplicates and analyzed by one-way ANOVA with Dunnett's multiple comparisons test.

-Figure 4O; Determination of relative RA concentrations in cells transfected with siNC or siALDH1A1. Data are shown as mean ± SD of technical triplicates and analyzed by unpaired t-test. ****$p < 0.0001$.

-Figure 5J; lines 1248-1252 in the figure legend; Representative images of PDO77, PDO76 and PDO80 treated with DMSO, Abemaciclib (1 μM), AGN (20 μM), AR7 (20 μM), or combination after 10 days culture (left). Scale bar = 200 μm. The matching scatter diagram shows data as mean ± SD of technical triplicates, one-way ANOVA

with Dunnett's multiple comparisons test (right). **p < 0.01, ***p < 0.001, ****p < 0.0001.

-Figure 6F-G; lines 1265-1267 in the figure legend; ChIP-qPCR analysis of RARα and ERα occupancy at genomic loci of ALDH1A1 in HEC-1-AP and HEC-1-AR, HEC-1-BP and HEC-1-BR cells. Data are presented relative to input, shown as mean ± SD of technical triplicates and analyzed by unpaired t-test.

-Figure 6H; lines 1268-1270 in the figure legend; Re-ChIP analysis shows the concurrent presence of both ERα and RARα at genomic loci of ALDH1A1 in HEC-1-AP and HEC-1-AR cells. Data are presented relative to input, showed as mean ± SD of technical triplicates and analyzed by t test.

-Figure 6I; lines 1270-1273 in the figure legend; ChIP-qPCR analysis of H3K27ac occupancy at genomic loci of ALDH1A1 in HEC-1-AR cells transfected with control siRNA, siRARA or siESR1. Data are shown as mean ± SD of technical triplicates and analyzed by unpaired t-test.

-Figure 6J; lines 1273-1276 in the figure legend; RT-qPCR validation of RARA and ALDH1A1 in HEC-1-AR and HEC-1-BR cells transfected with control siRNA or RARA siRNA. Data are shown as mean ± SD of technical triplicates and analyzed by unpaired t-test.

-Figure 6K; lines 1276-1278 in the figure legend; RT-qPCR validation of ESR1 and ALDH1A1 in HEC-1-AR and HEC-1-BR cells transfected with control siRNA or ESR1 siRNA. Data are shown as mean ± SD of technical triplicates and analyzed by unpaired t-test

-Figure 6M; lines 1281-1284 in the figure legend; ChIP qPCR analysis of H3K27ac, ERα and RARα occupancy at genomic loci of ALDH1A1 in HEC-1-AP cells treated with DMSO and RA (20 μM) for 72 hours. Data are presented relative to input, shown as mean ± SD of technical triplicates and analyzed by unpaired t-test.

-Figure 6N (up); lines 1284-1287 in the figure legend: RT-qPCR validation of ALDH1A1 in HEC-1-AP and HEC-1-BP cells treated with DMSO or RA (10 μM and 20 μM) (up). Data are shown as mean ± SD of technical triplicates and analyzed by one-way ANOVA with Dunnett's multiple comparisons test.

-Figure 7I; lines 1315-1317 in the figure legend: Determination of relative RA concentrations in PDX-EC1P and PDX-EC1R xenograft tumor tissues. Data are shown as mean ± SD of technical triplicates and analyzed by unpaired t-test.

Response to Reviewer: We are grateful to the Reviewer for the kind reminder. We apologized for the mistake in describing "technical triplicates" in the original legends. Actually, the experiments were repeated at least three times, and each biological repetition included three technical replicates. After verifying the consistency of technical triplicates, we calculated the mean value of technical triplicates from each independent experiment as the final data point for that sample.

We have corrected the descriptions in the figure legends as follows and updated the revised version of the manuscript. All the replicative data are shown in Source Data file.

In Figure 2I legend (Page 41): "RT-qPCR validation of ALDH1A1 in parental and resistant cells. Data are shown as mean ± SD of three independent experiments and analyzed by unpaired t-test. ***$p < 0.001$."
In Figure 2J legend (Page 41): "Data are presented relative to input, shown as mean ± SD of three independent experiments and analyzed by unpaired t-test. **$p < 0.01$, ***$p < 0.001$."
In Figure 3K legend (Page 43): "Representative images of PDO67, PDO76 and PDO77 treated with DMSO, Abemaciclib (1 μM), Dis (2 μM), dBET6 (2 μM), or combination after 10 days culture. The experiment was performed in three biological replicates. Scale bar = 200 μm. (left). The matching scatter diagram shows surface area of organoids, and one dot represents one organoid. Data are shown as mean ± SD and analyzed by Kruskal-Wallis with Dunn's multiple comparisons test. ***$p < 0.001$. (right)."
In Figure 4B legend (Page 43): "Data are shown as mean ± SD of three independent experiments and analyzed by unpaired t-test. ***$p < 0.001$."
In Figure 4C legend (Page 43): "Determination of relative vitA concentrations in cell culture medium at the indicated time points. Data are shown as mean ± SD of three independent experiments and analyzed by two-way ANOVA with Dunnett's multiple comparisons test, ***$p < 0.001$."
In Figure 4G legend (Page 44): "Resistant cells are treated with the indicated concentrations of Abemaciclib in B-27 supplement medium, vitA-deficient B-27 supplement medium or vitA-deficient B-27 supplement medium with vitA (10 μM). The number of viable cells is measured at 96 hours. Data are shown as mean ± SD of three independent experiments and analyzed by two-way ANOVA with Dunnett's multiple comparisons test, ***$p < 0.001$."
In Figure 4J legend (Page 44): "Relative ALDH enzyme activity between parental cells (HEC-1-AP and HEC-1-BP) and resistant cells (HEC-1-AR and HEC-1-BR). Data are shown as mean ± SD of three independent experiments and analyzed by unpaired t-test. ***$p < 0.001$."
In Figure 4L legend (Page 44): "Relative ALDH enzyme activity of indicated cells. Data are shown as mean ± SD of three independent experiments and analyzed by One-way ANOVA with Dunnett's multiple comparisons test. ns, not significant, ***$p < 0.001$."
In Figure 4N legend (Page 44): "Determination of relative RA concentrations in indicated cells. Data are shown as mean ± SD of three independent experiments and analyzed by one-way ANOVA with Dunnett's multiple comparisons test. ns, not significant, ***$p < 0.001$."
In Figure 4O legend (Page 44): "Determination of relative RA concentrations in cells transfected with siNC or si*ALDH1A1*. Data are shown as mean ± SD of three independent experiments and analyzed by one-way ANOVA with Dunnett's multiple comparisons test. ***$p < 0.001$."
In Figure 5K legend (Page 45): "Representative images of PDO77, PDO76 and PDO80 treated with DMSO, Abemaciclib (1 μM), AGN (20 μM), AR7 (20 μM), or combination after 10 days culture. Scale bar = 200 μm. (left). The matching scatter diagram shows

surface area of organoids, and one dot represents one organoid. Data are shown as mean ± SD and analyzed by Kruskal-Wallis with Dunn's multiple comparisons test. ***p < 0.001. (right)."

In Figure 6F-G legend (Page 46): "ChIP-qPCR analysis of RARα and ERα occupancy at genomic loci of *ALDH1A1* in HEC-1-AP and HEC-1-AR, HEC-1-BP and HEC-1-BR cells. Data are presented relative to input, shown as mean ± SD of three independent experiments and analyzed by unpaired t-test. *p < 0.05, **p < 0.01, ***p < 0.001."

In Figure 6H legend (Page 46): "Re-ChIP analysis shows the concurrent presence of both ERα and RARα at genomic loci of *ALDH1A1* in HEC-1-AP and HEC-1-AR cells. Data are presented relative to input, showed as mean ± SD of three independent experiments and analyzed by unpaired t-test. ***p < 0.001."

In Figure 6I legend (Page 46): "ChIP-qPCR analysis of H3K27ac occupancy at genomic loci of *ALDH1A1* in HEC-1-AR cells transfected with control siRNA, si*RARA* or si*ESR1*. Data are shown as mean ± SD of three independent experiments and analyzed by unpaired t-test."

In Figure 6J legend (Page 46): "RT-qPCR validation of *RARA* and *ALDH1A1* in HEC-1-AR and HEC-1-BR cells transfected with control siRNA or *RARA* siRNA. Data are shown as mean ± SD of three independent experiments and analyzed by one-way ANOVA with Dunnett's multiple comparisons. ***p < 0.001."

In Figure 6K legend (Page 46): "RT-qPCR validation of *ESR1* and *ALDH1A1* in HEC-1-AR and HEC-1-BR cells transfected with control siRNA or *ESR1* siRNA. Data are shown as mean ± SD of three independent experiments and analyzed by one-way ANOVA with Dunnett's multiple comparisons. **p < 0.01, ***p < 0.001."

In Figure 6M legend (Page 47): "ChIP qPCR analysis of H3K27ac, ERα and RARα occupancy at genomic loci of *ALDH1A1* in HEC-1-AP cells treated with DMSO and RA (20 μM) for 72 hours. Data are presented relative to input, shown as mean ± SD of three independent experiments and analyzed by unpaired t-test. **p < 0.01, ***p < 0.001."

In Figure 6N legend (Page 47): "RT-qPCR validation of *ALDH1A1* in HEC-1-AP and HEC-1-BP cells treated with DMSO or RA (10 μM and 20 μM) (up). Data are shown as mean ± SD of three independent experiments and analyzed by one-way ANOVA with Dunnett's multiple comparisons test. ***p < 0.001."

In Figure 7I legend (Page 48): "Determination of relative RA concentrations in PDX-EC1P and PDX-EC1R xenograft tumor tissues. Data are shown as mean ± SD of four biological replicates and analyzed by unpaired t-test. ***p < 0.001."

Reviewer #2 (Remarks to the Author):

I co-reviewed this manuscript with one of the reviewers who provided the listed reports. This is part of the Nature Communications initiative to facilitate training in peer review and to provide appropriate recognition for Early Career Researchers who co-review manuscripts.

Response to Reviewer: We highly appreciate the ECR co-review program. We thank the Reviewer for the positive comments and constructive suggestions. We believe that we have fully addressed the concerns in the point-by-point responses.

Reviewer #3 (Remarks to the Author):

The current paper addresses potential mechanisms of resistance to CDK4/6i therapy. Such small molecules are currently used in hormone receptor positive breast cancer and have therapeutic benefit. However, resistance remains an issue. Multiple mechanisms of resistance have been broadly described and most reflect non-genomic mechanisms. This paper provides evidence that increased expression of ALDH1A1 increases vitamin leading to increased retinoic acid accumulation. Critically, overexpression of ALDH1A1 was sufficient to drive resistance and it was critical for maintenance of resistance. RA accumulation led to increased RARa and ERa signaling that perpetuated ALDH1A1. This is an interesting model and much of the data was strong. However, there are significant issues that need to be addressed. The most significant of which is how SE are called from the genomic experiments. It is not described and it seems that enhanced H2K27ac is the only marker for SE. This is not fully justified and further it is unclear what or how SE were called; how much of an increase or clustering. Ultimately, while ALDH1A1 is up, it is far from clear that this reflects SE increase and further what drives this mechanism. Additional points follow.

Response to Reviewer: We appreciate the positive and insightful comments from the Reviewer, which have significantly enhanced the quality of our manuscript. There are three major concerns raised by the Reviewer: 1) The marker for SEs used in this study; 2) The definition of SEs in this study; 3) How ALDH1A1 is driving effects through super-enhancers.

1) The marker for SEs used in this study

Firstly, we identified the putative SEs based on H3K27ac marker in patient data and cell data for the consistency like multiple previous studies.(33-37) We agree with the reviewer that using H3K27ac alone may not be sufficient to define SEs. Specific histone modifications can distinguish between different categories of functional regulatory elements: H3K27ac and H3K4me1 with active enhancers.(33, 38, 39) It's more suitable to identify SEs by histone markers H3K27ac and H3K4me1. However, due to the limited availability of patient tumor samples, we only performed H3K27ac ChIP-seq on these samples.

To further accurately define the SE regions and identify SE-driven genes as the reviewer's suggestion, we re-identified the SEs in cell line models using the ChIP-seq data for two chromatin markers, including H3K27ac and H3K4me1. By integrating with patient data, we obtained similar results to previous version that *ALDH1A1* is an SE-driven gene. The revised Figure 2 is presented below (**Response Figure 10**):

Response Figure 10

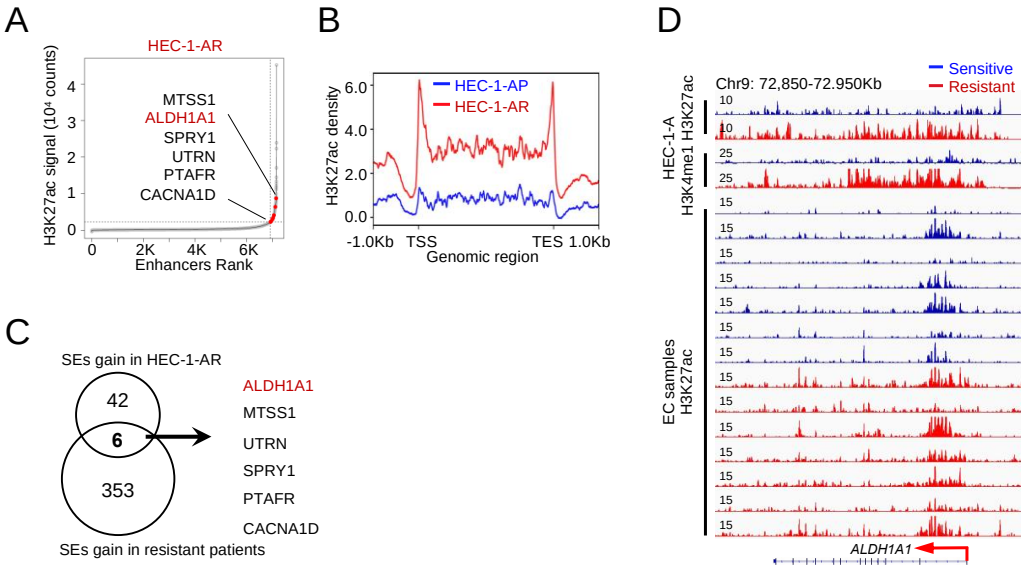

Response Figure 10. (A) Hockey-stick plots display rank order of H3K27ac ChIP-seq signals for the indicated SE-associated genes in HEC-1-AR cells. (B) Aggregate plots of H3K27ac chromatin landscapes flanking (±1 kb) de novo super-enhancer midpoints of gained SE in HEC-1-AP and HEC-1-AR cells. (C) Venn diagram shows the number and overlaps of SE-associated genes in resistant tumors and HEC-1-AR cells. (D) Tracks of ChIP-seq profiles (H3K27ac, H3K4me1) at the ALDH1A1 locus in sensitive and resistant tumors and cells.

2) The definition of SEs in this study

We apologize for not clearly stating the definition of SEs in the Methods section. SE regions in our study were defined based on the criteria described in previous studies.(33) Briefly, in patient samples, SE regions were identified using ROSE software (default parameters) with H3K27ac peak regions outside ±2.5 kb of all TSSs. In cell lines, SEs were called within H3K27ac+/ H3K4me1+ peak regions outside ±2.5 kb of all TSSs. The input-subtracted signal of each SE candidate was generated using bigWigAverageOverBed (sum of reads over covered bases). SE regions were ranked by the average H3K27ac ChIP-seq signal difference between sensitive and resistant groups. Gained SEs were those with average differential signals >0, and lost SEs were those with <0. This description has been supplemented and clarified in the Methods section of the revised manuscript.

In Method section (Page 30-31):

"**Identification of SE Regions**

SE regions in our study were defined based on the criteria described in previous studies.(33) Briefly, in patient samples, SE regions were identified using ROSE software (default parameters) with H3K27ac peak regions outside ±2.5 kb of all TSSs. In cell lines, SEs were called within H3K27ac+/H3K4me1+ peak regions outside ±2.5 kb of all TSSs. The input-subtracted signal of each SE candidate was generated using bigWigAverageOverBed (sum of reads over covered bases). SE regions were ranked

by the average H3K27ac ChIP-seq signal difference between sensitive and resistant groups. Gained SEs were those with average differential signals >0, and lost SEs were those with <0."

3) How ALDH1A1 is driving effects through super-enhancers

We also thank the Reviewer for raising this issue of how ALDH1A1 is driving effects through super-enhancers. We delineated the SE landscape and identified *ALDH1A1* as a SE-driven gene associated with CDK4/6i resistance. Mechanistically, we demonstrated that ALDH1A1 promotes RA accumulation and facilitates RARα/ERα-occupied SE-driven transcriptional activation of *ALDH1A1*. Based on these findings, we hypothesize that ALDH1A1 can modulate the activity of SEs, and the mechanism is dependent on RA-RAR axis (**Response Figure 11A**). First, we overexpressed ALDH1A1 in HEC-1-AP cells and found increased binding of H3K27ac, RARα and ERα at the *ALDH1A1* gene loci, which could be suppressed by RAR inhibition (AGN) (**Response Figure 11B**). Moreover, we knocked down ALDH1A1 expression and showed that the binding of H3K27ac, RARα and ERα at the ALDH1A1 gene loci was decreased, which could be significantly rescued by RA supplementation (**Response Figure 11C**). These results suggest that ALDH1A1-mediated CDK4/6i resistance is dependent on the positive feedback regulation of the RA-RAR signaling axis-driven SEs.

We have amended the descriptions in the Result section and Supplementary Figures as follows. In Result section (Page 16): "In addition, we found increased bindings of H3K27ac, RARα and ERα at the *ALDH1A1* gene loci in ALDH1A1-overexpressing cells, which could be suppressed by RAR inhibition (Supplementary Fig. 6I). Moreover, we knocked down ALDH1A1 expression and showed that the binding of H3K27ac, RARα and ERα at the ALDH1A1 gene loci was decreased, which could be significantly rescued by RA supplementation (Supplementary Fig. 6J). These results suggest that ALDH1A1-mediated CDK4/6i resistance is dependent on the positive feedback regulation of the RA-RAR signaling axis-driven SEs."

Finally, we believe that we have fully addressed all the additional points raised by the Reviewer in the point-by-point responses below.

Response Figure 11

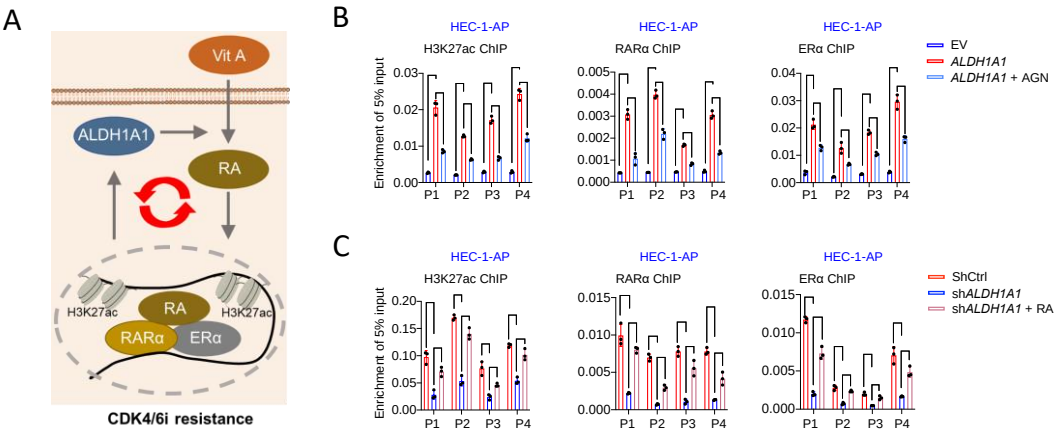

Response Figure 11. (A) Schematic model illustrates the role of ERα/RARα-ALDH1A1 positive feedback loop in inducing CDK4/6i resistance. ALDH1A1 was regulated by RA-mediated RARα/ERα-occupied SEs transcriptional activation, which in turn promoted vitA metabolism and RA production to activate *ALDH1A1* transcription. (B) ChIP-qPCR analysis of H3K27ac, ERα and RARα occupancy at genomic loci of *ALDH1A1* in HEC-1-AP cells overexpressing empty vector (EV) or ALDH1A1, or the latter treated with AGN (5 μM) for 72 hours. (C) ChIP-qPCR analysis of H3K27ac, ERα and RARα occupancy at genomic loci of *ALDH1A1* in HEC-1-AP cells expressing shCtrl or sh*ALDH1A1*, or the latter treated with RA (20 μM) for 72 hours. *$p < 0.05$, **$p < 0.01$, ***$p < 0.001$. One-way ANOVA with Dunnett's multiple comparisons test were used in Figure B-C.

1. How SE are called from the genomic experiments. It is not described and it seems that enhanced H2K27ac is the only marker for SE.

Response to Reviewer: We thank the Reviewer for pointing out this issue. For patient samples, SE regions were identified using ROSE referenced from previous studies(4). The input-subtracted signal for each SE was computed using bigWigAverageOverBed (sum of reads over covered bases). The SE regions were ranked by the average difference of sensitive/resistant samples H3K27ac ChIP-seq signals. Gained SEs were defined as regions that have average differential H3K27ac ChIP-seq signals >0. Lost SEs were defined as regions that have average differential H3K27ac ChIP-seq signals <0.

Moreover, we used two markers (H3K27ac and H3K4me1) to annotate SEs in cell line models. Through an integrated analysis of SE-driven genes from patient samples and cell lines, we identified *ALDH1A1* emerged as a SE gene related to CDK4/6i resistance. We addressed the description in the Method section in the update version.

In Method section (Page 30-31):

"**Identification of SE Regions**

SE regions in our study were defined based on the criteria described in previous studies.(33) Briefly, in patient samples, SE regions were identified using ROSE

software (default parameters) with H3K27ac peak regions outside ±2.5 kb of all TSSs. In cell lines, SEs were called within H3K27ac+/H3K4me1+ peak regions outside ±2.5 kb of all TSSs. The input-subtracted signal of each SE candidate was generated using bigWigAverageOverBed (sum of reads over covered bases). SE regions were ranked by the average H3K27ac ChIP-seq signal difference between sensitive and resistant groups. Gained SEs were those with average differential signals >0, and lost SEs were those with <0."

2. Through the paper, methods and experiments are not described with sufficient clarity to understand experimental procedures sufficiently to interpret data provided.

Response to Reviewer: We thank the Reviewer for pointing out this issue. In the updated version, we have supplemented the detailed descriptions of several methods, including the cell viability assay in cells and PDOs, establishment of acquired resistant cell lines or PDX models, establishment of PDOs, identification of SE regions.

In Materials and methods section (Page 22): "For the cell viability assay, cells were seeded in triplicate at the optimal density in 96-well plates. After 24-hour incubation, cells were divided into control groups and drugs-treated groups. The time-zero control groups refer to the groups in which ATP levels were measured at the beginning of the experiment, after cell attachment (prior to drug treatment). The control groups refer to cells cultured in complete medium containing only the vehicle (0.1% DMSO). The drug-treated groups refer to cells treated with the indicated drugs. For the control groups and drug-treated groups, cells were cultured at 37 ºC and ATP levels were measured after 96 hours. The number of viable cells was measured using the Cell Titer-Glo Luminescent Cell Viability Assay (#G7573, Promega, Madison, WI), according to the manufacturer's instructions."

In Materials and methods section (Page 22-23):

"**Establishment of cell lines with acquired resistance to Abemaciclib**

Cells were grown with progressively increasing concentrations of Abemaciclib. Subconfluent cells were treated with Abemaciclib at IC50 doses (based on 96-hour cytotoxicity assays) for two 3-day periods, and surviving cells were maintained for another 4 days. The process was repeated once, and the remaining cells were cultured in the presence of drug for 3 additional passages. Resistant cells were maintained in the presence of Abemaciclib, and the same passage parental cells were treated with the same dose of DMSO."

In Materials and methods section (Page 23-24): "

"For the cell viability assay, organoids were harvested and dissociated using TrypLE™ Express (Gibco, 12604013) for 10 min at 37 ºC. The dissociated PDOs were resuspended in ice-cold MAcreGel (Mingao Biotech) and seeded into a 96-well plate (Corning). After allowing the MAcreGel drops to solidify for 15 min at 37 ºC, PDOs were overlaid with endometrial cancer organoid medium containing the indicated doses of drugs. Five days after drug treatment, cell viability was measured using the Cell Viability ATP Assay Kit (Mingao Biotech) according to the manufacturer's instructions on a Spark microplate reader (Tecan)."

In Materials and methods section (Page 30-31):

"**Identification of SE Regions**

SE regions in our study were defined based on the criteria described in previous studies.(33) Briefly, in patient samples, SE regions were identified using ROSE software (default parameters) with H3K27ac peak regions outside ±2.5 kb of all TSSs. In cell lines, SEs were called within H3K27ac+/H3K4me1+ peak regions outside ±2.5 kb of all TSSs. The input-subtracted signal of each SE candidate was generated using bigWigAverageOverBed (sum of reads over covered bases). SE regions were ranked by the average H3K27ac ChIP-seq signal difference between sensitive and resistant groups. Gained SEs were those with average differential signals >0, and lost SEs were those with <0."

In Materials and methods section (Page 32): "The method of establishment Abemaciclib acquired resistant PDX was reference from previous studies. (40) We firstly constructed PDXs with female NOD-SCID mice (5-8 weeks old), which were purchased from GemPharmatech (Nanjing, China) and housed in the Biological Resource Centre. When tumors reached 70 mm^3, PDXs were treated with Abemaciclib (30 mg/kg, every 2-3 days, oral gavage). Tumor growth was monitored and would be excised upon reaching 1,000 mm^3. The excised tumor tissue was minced with a sterile scalpel into patches and implanted subcutaneously for passage into the next generation of PDXs. The process was repeated, and the PDXs were fed in the presence of drug for 3 additional passages. Resistant PDXs were maintained in the presence of Abemaciclib, and the same passage sensitive PDXs were treated with vehicle (saline)."

3. Why are the authors observing cell death with CDK4/6i? These are cytostatic drugs that trigger quiescence or ultimately senescence. This is a flaw…if death is observed, it suggests off target effects, given that in vivo death generally reflects recruitment of cytotoxic immune cells.

Response to Reviewer: We thank the review for pointing out this issue. We agree with the reviewer that the canonical role of CDK4/6i lies in inducing quiescence/senescence.(41) It's known that the loss of RB1 correlates with CDK4/6i resistance in multiple models.(42-44) RB1 loss-mediated molecular alterations may render cancer cells vulnerable to specific drug, thereby promoting the induction of apoptosis.(45) CDK4/6i can only induce senescence in sensitive cells but not in resistant cells, while combination treatment with a BRD4 inhibitor elicits a strong induction of apoptosis in RB1-knockout resistant cells (**Response Figure 12A**).(46) The expression levels of RB1 were also significantly decreased in our resistant cell models (**Response Figure 12B**). Consistently，we obtained the similar results that combination treatment but not CDK4/6i alone could induce significant cleaved PARP and cleaved caspase-3 in resistant cells (**Figure 3C, 3H, 5J**). Furthermore, multiple studies in demonstrating that combination treatment of CDK4/6i with other drugs significantly induced cell death (47-49), while single drug treatment with CDK4/6i could not exert significant induction of cleaved PARP and cleaved caspase-3

(**Response Figure 12C-E**). Taken together, these data support the specific role of CDK4/6i in mediating cell death.

We have cited and discussed these findings in the Result section as follows (Page 9): "Previous studies showed CDK4/6i can only induce senescence in sensitive cells but not in resistant cells, while combination treatment with a BRD4 inhibitor elicits a strong induction of apoptosis in RB1-knockout resistant cells.(46) The expression levels of RB1 were also significantly decreased in our resistant cell models (Supplementary Fig. 3C). We obtained similar results that combined CDK4/6i with Disulfiram, but not CDK4/6i alone, induced significant cleaved PARP and caspase-3 in resistant cells, whereas no significant senescence was observed (Figure 3C, Supplementary Fig. 3D)."

Response Figure 12

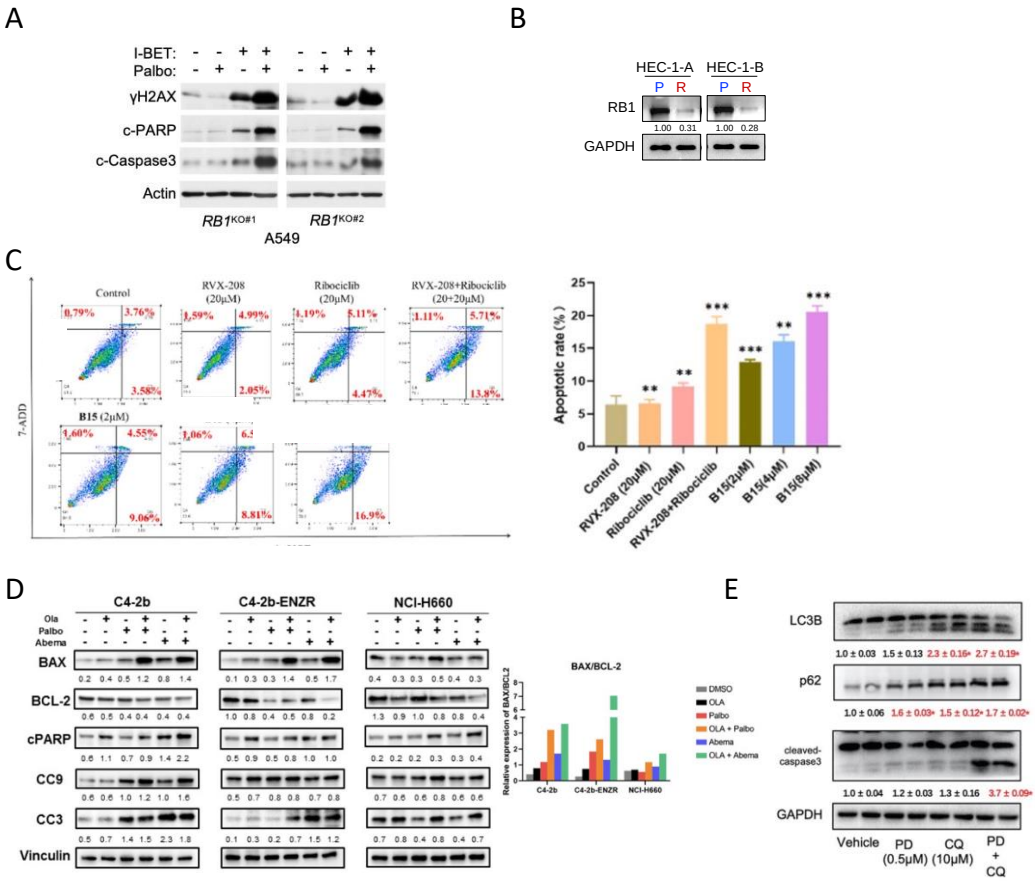

Response Figure 12. (A) From Figure 6G in Zhu X et al.'s work (PMID: 38277141). (B) Immunoblot analysis of indicated cells with RB1 and GAPDH. (C) From Figure 9A and Figure 9C in Zhang Y et al.'s work (PMID: 40101452). (D) From Figure 1H in Cheng Wu et al.'s work (PMID: 34158347). (E) From Figure 4E in Wen Y et al.'s work (PMID: 39136283).

4. No description of proliferation assays. Is cell doubling measured? Or is this a metabolic assay used as a surrogate. If the latter, this is not valid given that CDK4/6 regulate cell metabolism independently of cell division.

Response to Reviewer: We thank the Reviewer for pointing out this issue. Consistent with multiple previous studies in which ATP assays have been commonly used to verify the proliferation-regulating effects of CDK4/6i (20, 46, 50-53), we also utilized ATP assays as proliferation assays methods.

We measured cell doubling by ATP levels after 96 hours of drugs treatment, using time-zero control groups or Vehicle control groups to normalization. In Fig. 3E, 4G, 5H, Supplementary Fig. 2A, 2C and 3B, cells were divided into Vehicle control groups and drugs treated groups, and ATP levels in all groups were measured after 96 hours. In Supplementary Fig. 3A, 3D and 3F, cells were divided into time-zero control groups and drugs treated groups. ATP levels in time-zero control groups were measured at the beginning of the experiment, after cell attachment (prior to drug treatment), and ATP levels in drugs treated groups were measured at the indicated days.

In addition, we also validated our findings in other models, including colony formation assays and PDOs models. We performed colony formation assays to directly evaluate long-term cell proliferation and conducted manual cell counting in organoid models to directly reflect changes in viable cell numbers. These two non-metabolism-dependent direct methods are highly consistent with the ATP results.

The detailed procedures of ATP assays have now been amended in Methods section in the updated revision (Page 22): "For the cell viability assay, cells were seeded in triplicate at the optimal density in 96-well plates. After 24-hour incubation, cells were divided into control groups and drugs-treated groups. The time-zero control groups refer to the groups in which ATP levels were measured at the beginning of the experiment, after cell attachment (prior to drug treatment). The control groups refer to cells cultured in complete medium containing only the vehicle (0.1% DMSO). The drug-treated groups refer to cells treated with the indicated drugs. For the control groups and drug-treated groups, cells were cultured at 37 ºC and ATP levels were measured after 96 hours. The number of viable cells was measured using the Cell Titer-Glo Luminescent Cell Viability Assay (#G7573, Promega, Madison, WI), according to the manufacturer's instructions."

5. The authors need to measure cell senescence with single drug and combinations.

Response to Reviewer: We appreciate the constructive suggestions from the Reviewer. We conducted the cell senescence experiment by detecting the level of senescence-associated β-galactosidase (Senescence β-Galactosidase Staining Kit, C0602, Beyotime, China). The results indicated that there is no significant change in senescent cells in either the combination group or other groups (**Response Figure 13A**), which is consistent with the previous report that combination treatment with Palbociclib and BRD4 inhibitor effectively induced cell death but not senescence in CDK4/6i resistant models (**Response Figure 13B**).(46)

We have cited and discussed these findings in the discussion section as follows (Page 9): "Previous studies showed CDK4/6i can only induce senescence in sensitive cells but not in resistant cells, while combination treatment with a BRD4 inhibitor elicits a strong induction of apoptosis in RB1-knockout resistant cells.(46) The expression

levels of RB1 were also significantly decreased in our resistant cell models (Supplementary Fig. 3C). We obtained similar results that combined CDK4/6i with Disulfiram, but not CDK4/6i alone, induced significant cleaved PARP and caspase-3 in resistant cells, whereas no significant senescence was observed (Figure 3C, Supplementary Fig. 3D)."

Response Figure 13

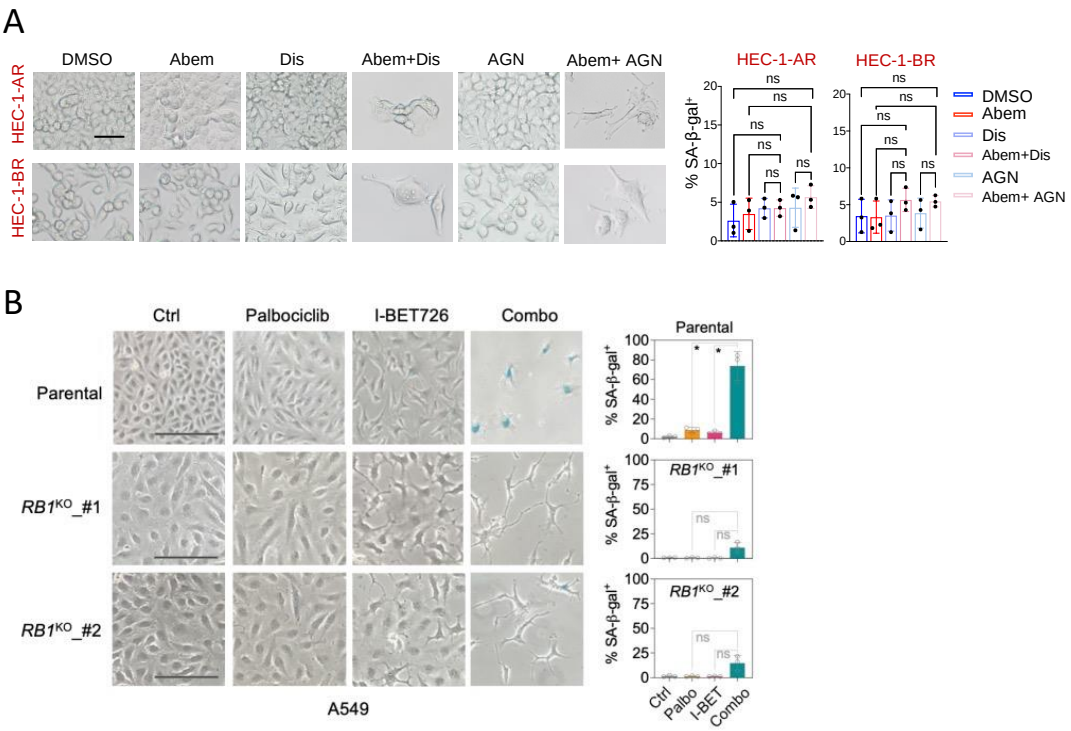

Response Figure 13. (A) Representative image and quantification of SA-β-gal positive cells in HEC-1-AR and HEC-1-BR cells treated with DMSO, Abemaciclib (0.5 μM), Disulfiram (1 μM for HEC-1-AR and 2 μM for HEC-1-BR), AGN (5 μM for HEC-1-AR and 10 μM for HEC-1-BR), or combination. Scale bar = 50 μm. One-way ANOVA with Dunnett's multiple comparisons test were used. ns, not significant. (B) From Figure 4I-J in Zhu X et al.'s work (PMID: 38277141).

6. In figure 4 the authors state that resistant cell "outcompete" parental cells. This experiment as described does not address competition. It simply demonstrates that resistant cells utilize more Vit A than parental.

Response to Reviewer: We thank the Reviewer for pointing out this issue. We have amended the description in the updated version In Result section (Page 11): "By detecting the vitA levels in cell culture medium from parental and resistant cells, we found that the abundance of vitA in resistant cells was decreased, and this decline occurred even more rapidly than in parental cells over time (Fig. 4C), indicating that resistant cells utilize more vitA than parental cells."

7. How were doses of Vit A and RA? Dose response? From Literature? No description.

Response to Reviewer: We thank the Reviewer for pointing out this issue. We used 20 μM RA in Figure 4D and Figure 6M, and 10 μM VitA in Figure 4E and Figure 4G. We first determined the drug concentrations based on literature reports: previous studies have indicated that 20 μM RA was used in MDA-MB-231 cells without affecting cell viability(8), and Colucci M et al. treated RWPE-1 and 22RV1 cells with 10 μM VitA in their project.(13)

Additionally, our preliminary experiments demonstrated that the effects of RA and VitA are dose-dependent. The results showed that 20 μM RA and 10 μM VitA exerted the most pronounced effects in mediating CDK4/6 inhibitor resistance, accompanied by a significant increase in ALDH1A1 expression levels. Furthermore, cellular viability remained unaffected (**Figure 6N, Response Figure 14**). Therefore, we used 20 μM RA and 10 μM VitA for further experiments. We have amended the description in the Result section and Supplementary Figure 4 in the updated version.

In Result section (Page 11): "Moreover, the effects of RA and vitA in mediating the Abemaciclib resistance became more pronounced as their concentrations increased (Supplementary Fig. 4E-F)."

Response Figure 14

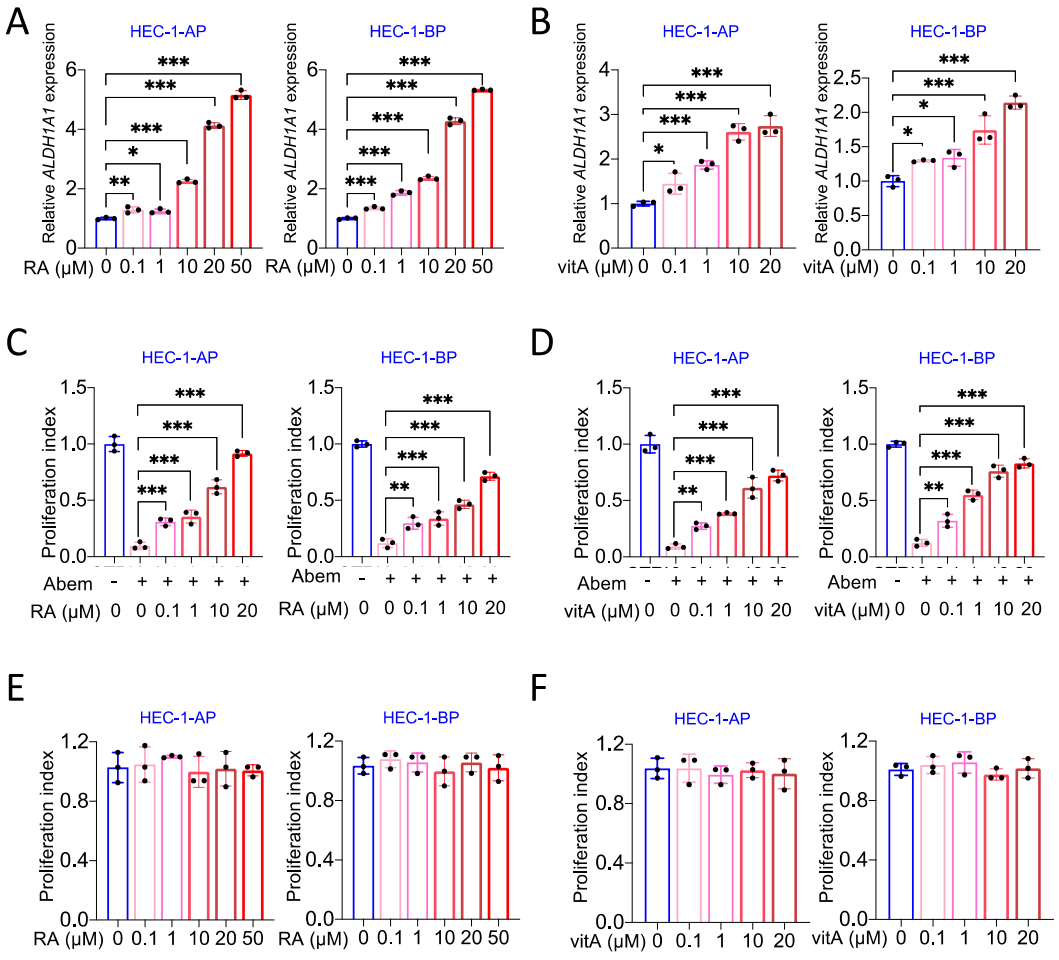

Response Figure 14. (A-B) RT-qPCR validation of ALDH1A1 in HEC-1-AP and HEC-1-BP cells treated with DMSO, RA (0.1 μM, 1 μM, 10μM, 20 μM and 50 μM) or vitA (0.1 μM, 1 μM, 10 μM and 20 μM). Data are shown as mean ± SD of and analyzed by one-way ANOVA with Dunnett's multiple comparisons test. (C-D) HEC-1-AP and HEC-1-BP cells treated with combinations of RA (0 μM, 0.1 μM, 1 μM, 10 μM and 20 μM) and Abemaciclib (0.5 μM), or combinations of vitA (0 μM, 0.1 μM, 1 μM, 10 μM and 20 μM) and Abemaciclib (0.5 μM). The number of viable cells is measured at 96 hours. Data are shown as mean ± SD and analyzed by one-way ANOVA with Dunnett's multiple comparisons test. (E-F) HEC-1-AP and HEC-1-BP cells treated with RA (0 μM, 0.1 μM, 1 μM, 10 μM and 20 μM) and the number of viable cells is measured at 96 hours. Data are shown as mean ± SD. *$p < 0.5$, **$p < 0.01$, ***$p < 0.001$.

8. In figure 5, all conclusions are based on RNA-seq. Transcription does not necessarily reflect translation. The authors need to demonstrate that increases observed by RNA-seq are reflected at the protein level.

Response to Reviewer: We thank the Reviewer for the constructive advice. To reflect the changes in the protein levels of these genes, we performed immunoblot analysis and found that multiple representative RA signaling targets, including ALDH1A1, ALDH1A3, DLAT, DLD, DUSP6 and PTPRH, were significantly downregulated following ALDH1A1 knockdown in both HEC-1-AR and HEC-1-BR cells, which is consistent with RNA-seq results in Fig. 5D (**Response Figure 15**). We have revised the descriptions in the Result section and Supplementary Figure 5B in the updated version.

In Result section (Page 12-13): "Multiple representative RA signaling targets were significantly downregulated following ALDH1A1 knockdown in both HEC-1-AR and HEC-1-BR cells (Fig. 5D, Supplementary Fig. 5A-B)."

Response Figure 15

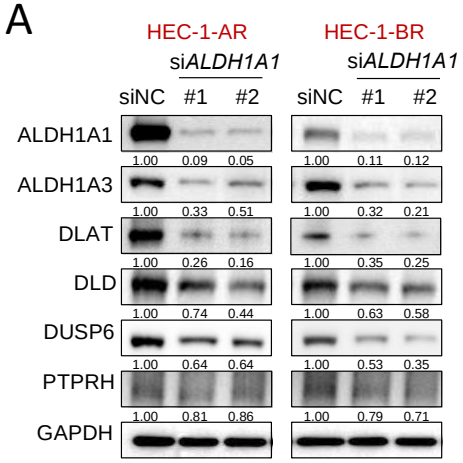

Response Figure 15. (A) Immunoblot analysis of ALDH1A1, ALDH1A3, DLAT, DLD, DUSP6 and PTPRH in HEC-1-AR and HEC-1-BR cells transfected with control siRNA or *ALDH1A1* siRNA.

Reviewer #4 (Remarks to the Author):

The manuscript entitled “Targeting Super-Enhancer-1 Driven ALDH1A1-RARα/ERα Feedback Loop to Mitigate CDK4/6 Inhibitor Resistance via Suppression of Vitamin A Metabolism” by Chen et al. addresses mechanisms of resistance to CDK4/6 inhibitors (CDK4/6i), an important clinical problem. Inhibitors of CDK4/6 activity have shown promise in the clinic and palbociclib, abemaciclib, and ribociclib are FDA-approved for use in patients. However, the therapeutic promise of these agents is dampened by inevitable emergence of resistance. The authors present a compelling study in which they identify a novel mechanism of CDK4/6i resistance involving epigenetic alterations. The study is predominantly performed in endometrial cancer (EC) models, although data from breast cancer cells are also presented. Integration of transcriptomic and chromatin data (RNA-seq and ChIP-seq data) from sensitive and resistant EC organoids and EC cell lines identified ALDH1A1 as a super enhancer-driven gene associated with CDK4/6i resistance. The authors delineate a novel positive feedback axis that promotes CDK4/6i resistance in which increased levels of ALDH1A1 accumulate in resistant cells, promoting vitamin A metabolism, accumulation of retinoic acid, interaction between RARα and ERα in the nucleus, and RARα/ERα-occupied super enhancer-driven transcriptional activation of ALDH1A1. They further determined that ALDH1A1 can be epigenetically silenced with BRD4 inhibitors to mitigate CDK4/6i resistance. Based on their findings, the authors propose that inhibition of this novel axis (e.g., ALDH1A1 inhibition) is a promising approach to re-sensitize tumors to CDK4/6i. The data are generally of good quality and supportive of the conclusions of the authors. While the study should be of interest to the broad readership of Nature Communications, the following issues should be addressed.

Response to Reviewer: We appreciate the positive comments and constructive suggestions from the Reviewer. We believe that we have fully addressed the concerns in the point-by-point responses below.

General:

1) In many cases (e.g., colony formation assays, Western blots), the number of biological replicates performed is not clear. While technical replicates are indicated, the number of times the experiment was carried out with similar results is not specified. This should be corrected throughout the manuscript.

Response to Reviewer: We thank the Reviewer for pointing out this issue. We apologized for that the term “technical triplicates” was mistakenly used in the original legends when referring to “biological triplicates”. All of our experiments were performed at least three times as independent experiments and for each independent experiment, technical triplicates were performed to ensure detection accuracy. We have corrected the descriptions in the figure legend and amended the number of biological

replicates for all experiments in the revised version of the manuscript. All the data are shown in the Source Data file.

2) Western blot data should be quantified, especially in experiments where changes are modest.

Response to Reviewer: We thank the Reviewer for pointing out this issue. We quantified the blots using ImageJ/Fiji software (https://fiji.sc/) and have amended the data in Figure 2L, 3A, 3C-D, 3H-J, 4K, 5I, 6A, 6L and 6N, and have revised the descriptions Method section in the updated version.

In Method section (Page 24): "The blots were quantified using ImageJ/Fiji software (https://fiji.sc/)."

3) Information on the characteristics of the 16 endometrial cancer organoids generated should be provided. Were there any trends regarding the response of these organoid lines to CDK4/6i based on EC type, grade, etc?

Response to Reviewer: We thank the Reviewer for pointing out this issue. We have provided the characteristics of the 16 endometrial cancer patients in Table S1 in the updated version.

Regarding the response of these 16 corresponding PDOs to CDK4/6i, we performed statistical analysis and the result showed no statistical difference between sensitive group and resistant group based on age, EC stage, grade and histopathology (**Response Table 1**). We have updated Table S1 in the revised version.

Response Table 1. Clinicopathologic features of study patients.

Characteristic	Sensitive	Resistant	*p*	All cases
Number of patients	8	8	-	16
Age at the time of surgery, yrs	55.50 ± 10.81	57.87 ± 10.56	0.663	56.69 ± 10.40
2023 FIGO Stage, n (%)			0.426	
Stage I	4 (25.00%)	7 (43.75%)		11(68.75%)
Stage II	1 (6.25%)	1 (6.25)		2 (12.50%)
Stage III	2 (12.50%)	0 (0%)		2 (12.50%)
Stage IV	1 (6.25%)	0 (0%)		1 (6.25%)
Grade, n (%)			0.804	
Grade 1	1 (6.25%)	3 (18.75%)		4(25.00%)
Grade 2	5 (31.25%)	3 (18.75%)		8 (50.00%)
Grade 3	2 (12.50%)	2 (12.50%)		4 (25.00%)
Histopathology, n (%)			1	
Endometrioid carcinoma	7 (43.75%)	7 (43.75%)		14 (87.50%)
Others	1 (6.25%)	1 (6.25%)		2 (12.50%)
Estrogen receptor, ER, n (%)			-	

positive	8 (50.00%)	8 (50.00%)		16 (100%)
negative	0 (0%)	0 (0%)		0 (0%)
Progesterone receptor, PR, n (%)			-	
positive	8 (50.00%)	8 (50.00%)		16 (100%)
negative	0 (0%)	0 (0%)		0 (0%)

4) Experimental details on how CDK4/6i-resistant EC cells and PDXs were generated (e.g., drug concentrations, duration of treatment at each concentration) should be included in the Materials and Methods.

Response to Reviewer: We thank the advice from the Reviewer. We have supplemented the detailed experimental process on how CDK4/6i-resistant EC cells and PDXs were generated in the Method section in the updated version as follows:

The generation of CDK4/6i-resistant EC cells (Page 22-23):

"**Establishment of cell lines with acquired resistance to Abemaciclib**

Cells were grown with progressively increasing concentrations of Abemaciclib. Subconfluent cells were treated with Abemaciclib at IC50 doses (based on 96-hour cytotoxicity assays) for two 3-day periods, and surviving cells were maintained for another 4 days. The process was repeated once, and the remaining cells were cultured in the presence of drug for 3 additional passages. Resistant cells were maintained in the presence of Abemaciclib, and the same passage parental cells were treated with the same dose of DMSO."

The generation of CDK4/6i-resistant EC PDXs (Page 32): "The method of establishment Abemaciclib acquired resistant PDX was reference from previous studies. (40) We firstly constructed PDXs with female NOD-SCID mice (5-8 weeks old), which were purchased from GemPharmatech (Nanjing, China) and housed in the Biological Resource Centre. When tumors reached 70 mm^3, PDXs were treated with Abemaciclib (30 mg/kg, every 2-3 days, oral gavage). Tumor growth was monitored and would be excised upon reaching 1,000 mm^3. The excised tumor tissue was minced with a sterile scalpel into patches and implanted subcutaneously for passage into the next generation of PDXs. The process was repeated, and the PDXs were fed in the presence of drug for 3 additional passages. Resistant PDXs were maintained in the presence of Abemaciclib, and the same passage sensitive PDXs were treated with vehicle (saline)."

5) All the experiments were performed using a single CDK4/6i inhibitor (abemaciclib) and results are expected to apply to other clinically relevant CDK4/6i. If possible, confirmation that the pathway is present in tumor cells that are resistant to another FDA-approved CDK4/6i would strengthen the study.

Response to Reviewer: We thank the Reviewer for pointing out this issue. We have performed some experiments in the resistant cells with another FDA-approved CDK4/6i (Palbociclib), which showed the same results as those with Abemaciclib

(**Response Figure 16**). We have updated the data in the Supplementary Fig. 1A-B, Supplementary Fig. 2B Supplementary Fig. 3B, Supplementary Fig. 4D, and Supplementary Fig. 4G in the revised version.

Response Figure 16

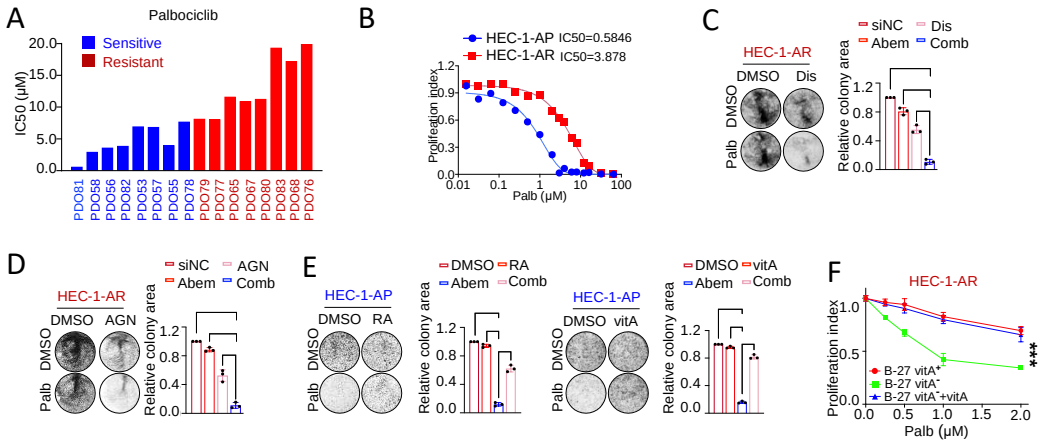

Response Figure 16. (A) Growth-inhibitory effect of 16 PDOs treated with different doses of Palbociclib. (B) HEC-1-AP and HEC-1-AR cells treated with the indicated concentrations of Palbociclib. The number of viable cells is measured at 96 hours. IC50 values for HEC-1-AP and HEC-1-AR cells at exposure durations of 96 hours to Palbociclib are shown. Data are represented the mean of three independent replicates. (C) Representative images and quantification of colony formation assay of resistant cells treated with DMSO, Palbociclib (1 μM), Disulfiram (1 μM), or combination for 72 hours. Data are shown as mean ± SD of three independent experiments and analyzed by One-way ANOVA with Dunnett's multiple comparisons test. ***$p < 0.001$. (D) Representative images and quantification of colony formation assay of resistant cells treated with DMSO, Palbociclib (1 μM), AGN (5 μM), or combination. Data are shown as mean ± SD of three independent experiments and analyzed by One-way ANOVA with Dunnett's multiple comparisons test. ***$p < 0.001$. (E) Representative images and quantification of colony formation assay of HEC-1-AP cells treated with DMSO, RA (20 μM)/vitA (10 μM), Palbociclib (0.5 μM), or combination. Data are shown as mean ± SD of three independent experiments and analyzed by One-way ANOVA with Dunnett's multiple comparisons test. ***$p < 0.001$. (F) Resistant cells are treated with the indicated concentrations of Palbociclib in B-27 supplement medium, vitA-deficient B-27 supplement medium or vitA-deficient B-27 supplement medium with vitA (10 μM). The number of viable cells is measured at 96 hours. Data are shown as mean ± SD of three independent experiments and analyzed by two-way ANOVA with Dunnett's multiple comparisons test, ***$p < 0.001$.

6) There are many languages and grammatical errors throughout the manuscript that need to be addressed.

Response to Reviewer: We thank the Reviewer for the kind advice. We have carefully proofread the entire manuscript to correct any linguistic and grammatical errors. Additionally, the manuscript has been reviewed and polished by a professional professor with expertise in life sciences. All revisions are marked in red in the updated version. Should any linguistic problems still be identified, we will address them promptly to meet the journal's requirements.

Specific Comments:

1) Fig. 3I and 3J: Near complete knockdown of BRD4 resulted in modest downregulation of ALDH1A1. Can the authors comment on other potential mediators of ALDH1A1 accumulation in CDK4/6i resistant cells?

Response to Reviewer: We thank the Reviewer for pointing out this issue. Firstly, we have supplemented quantitative analysis of WB band intensities (normalized to internal reference GAPDH) in the updated version. The results showed that the knockdown efficiency of BRD4 in HEC-1-AR cells was ~60%-75% (not fully complete), and ALDH1A1 expression was stably downregulated by ~30%-50%. Indeed, the concordance between BRD4 knockdown efficiency and ALDH1A1 downregulation was more pronounced in HEC-1-BR cells (**Response Figure 17A**). This finding demonstrated that even partial BRD4 knockdown induces a detectable reduction in ALDH1A1 expression. Secondly, in Fig 3I, the results showed that dBET6 and JQ1 treatment could repress expression of ALDH1A1 in a dose-dependent manner (**Response Figure 17B**). Given that both dBET6 and JQ1 are bromodomain-inhibiting agents targeting not only BRD4 but also BRD2 and BRD3 (54), it is plausible that other BET family members may sustain ALDH1A1 expression following BRD4 knockdown, which warrants further investigation in the future.

Response Figure 17

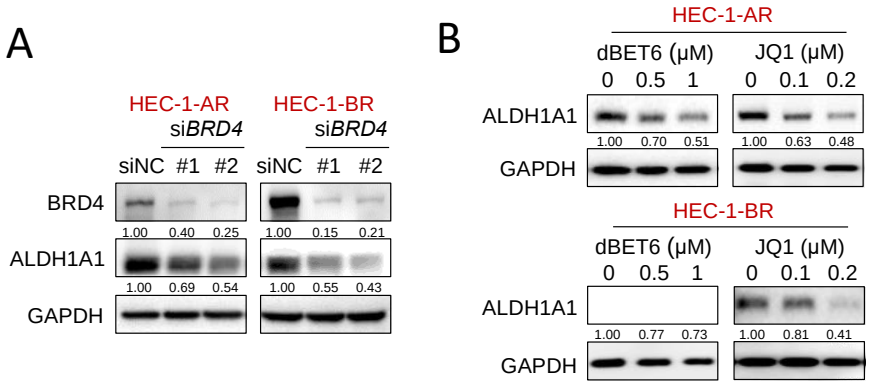

Response Figure 17. (A) Immunoblot analysis of ALDH1A1 expression in HEC-1-AR and HEC-1-BR cells transfected with control siRNA or *BRD4* siRNA for 72 hours. Shown are representative blots from three independent experiments. (B) Immunoblot

analysis of ALDH1A1 expression in HEC-1-AR and HEC-1-BR cells treated with BRD4 inhibitors (dBET6 and JQ1) for 72 hours. Shown are representative blots from three independent experiments.

2) Figs. 3K and 5J: A larger scale should be used on the y-axis to clarify the observed effects.

Response to Reviewer: We thank the constructive advice from the Reviewer. To clarify the observed effects, we have adjusted the colors and modified the scale in the updated version as follow (**Response Figure 18**).

Response Figure 18

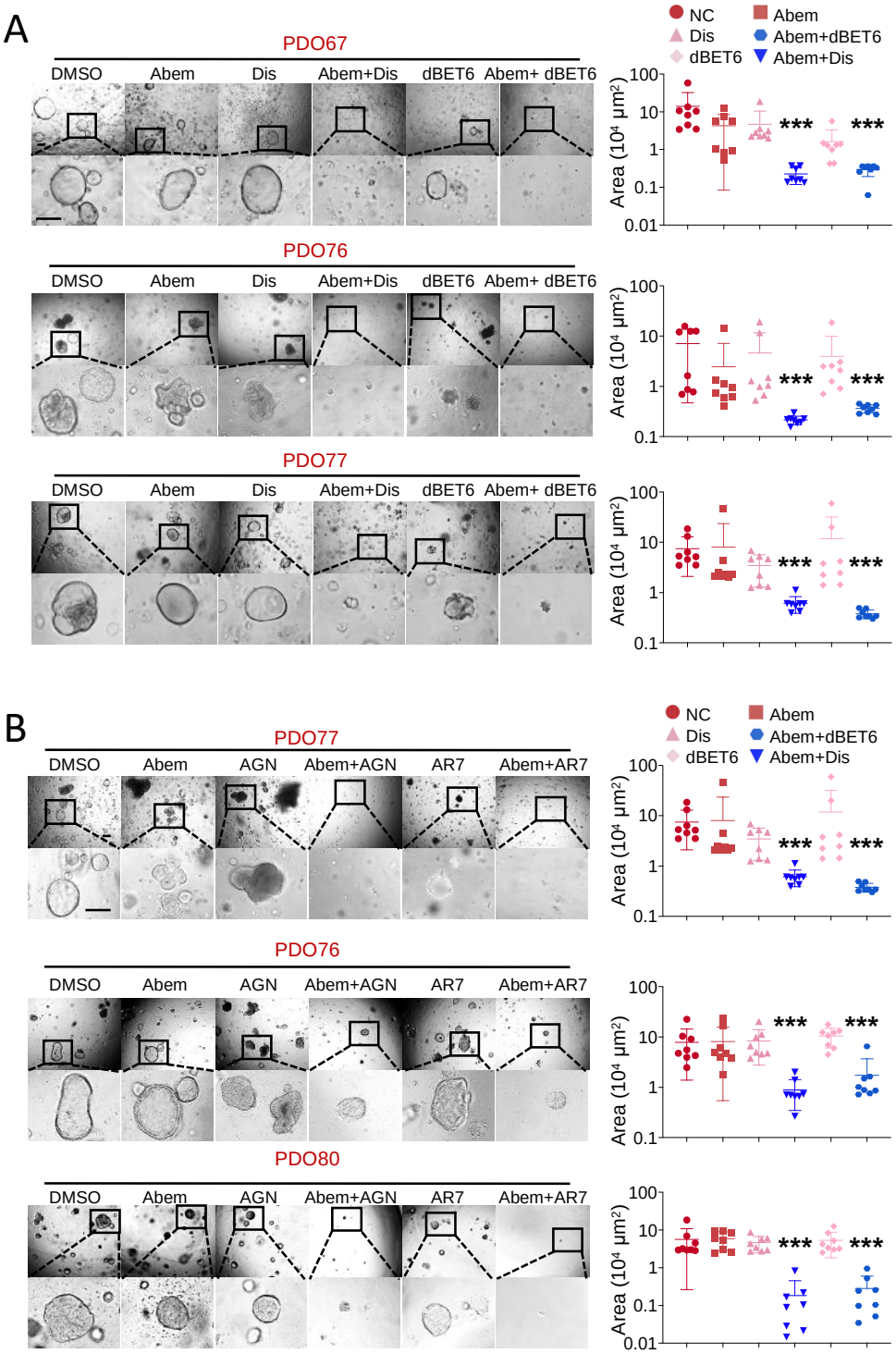

Response Figure 18. (A) Representative images of PDO67, PDO76 and PDO77 treated with DMSO, Abemaciclib (1 µM), Dis (2 µM), dBET6 (2 µM), or combination after 10 days culture. The experiment was performed in three biological replicates. Scale bar = 200 µm. (left). The matching scatter diagram shows surface area of organoids, and one dot represents one organoid. Data are shown as mean ± SD and analyzed by Kruskal-Wallis with Dunn's multiple comparisons test. ***$p < 0.001$. (right). (B) Representative

images of PDO77, PDO76 and PDO80 treated with DMSO, Abemaciclib (1 μM), AGN (20 μM), AR7 (20 μM), or combination after 10 days culture. Scale bar = 200 μm. (left). The matching scatter diagram shows surface area of organoids, and one dot represents one organoid. Data are shown as mean ± SD and analyzed by Kruskal-Wallis with Dunn's multiple comparisons test. ***$p < 0.001$. (right).

3) The data in Fig. 4M are not compelling.

Response to Reviewer: We thank the Reviewer for the key suggestions. We performed three times of independent experiments, with results as shown in the figure below (**Response Figure 19**). The data in Fig. 4M has now been replaced with a clearer, more representative one in the updated manuscript. Furthermore, we performed quantitative analysis of the colonies using ImageJ/Fiji software (https://fiji.sc/), which further substantiated our conclusions that only wide-type ALDH1A1, rather than the mutant, could confer resistance to Abemaciclib. The results from all three replicate experiments have been uploaded to the source data file.

Response Figure 19

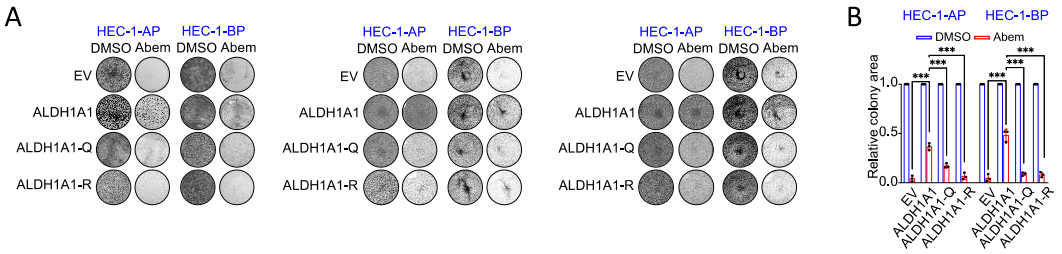

Response Figure 19. (A-B) Colony formation assay of cells treated with DMSO or Abemaciclib (0.5 μM) in wide-type or K193Q/R-mutant ALDH1A1-overexpressing cells (left). The number of colonies was counted. Data are presented as mean ± SD (n = 3) and analyzed by One-way ANOVA with Dunnett's multiple comparisons test. ***$p < 0.001$.

4) Some of the data in Fig. 5I are not convincing (e.g., HEC-1-AR cl-Cas3). Blots of better quality should be provided and quantified.

Response to Reviewer: We thank the constructive advice from the Reviewer. We have updated a more convincing image and quantified the blots using ImageJ/Fiji software (https://fiji.sc/). The high-resolution images of blot were shown as follows (**Response Figure 20**).

Response Figure 20

A

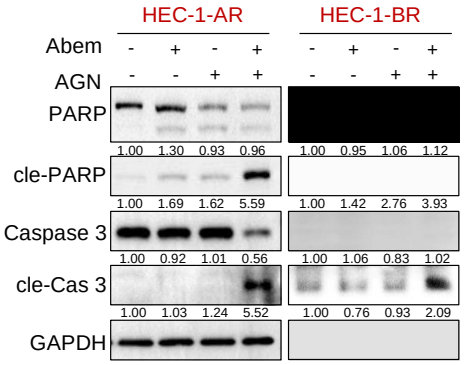

Response Figure 20. (A) Immunoblot analysis of PARP, cleaved-PARP, Caspase 3 and cleaved-Caspase 3 in HEC-1-AR and HEC-1-BR cells treated with Abemaciclib (0.5 μM), AGN (10 μM for HEC-1-AR and 20 μM for HEC-1-BR), or combination for 72 hours. Shown are representative blots from three independent experiments.

5) The graph on the right in Fig. 7A appears to be mislabeled.

Response to Reviewer: We thank the Reviewer for pointing out the mistake in our Figure. We have amended this point in the updated version (**Response Figure 21**).

Response Figure 21

A

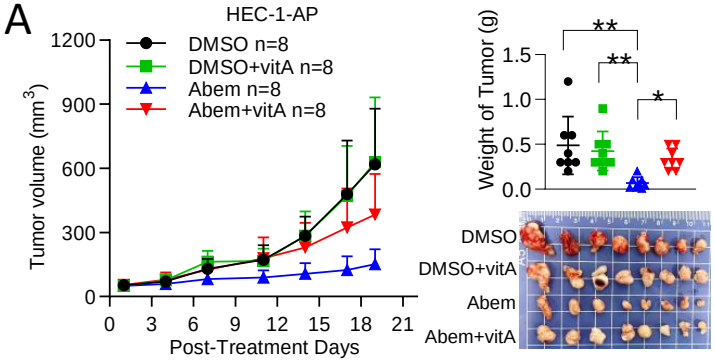

Response Figure 21. (A) The growth curve of tumor volume with DMSO, high vitA diet, Abemaciclib, or combination in HEC-1-AP xenografts, error bars represent ± SD. (left). Weight of tumors and the image of tumors with indicated treatment in HEC-1-AP xenografts. (right).

6) In Fig. 7B, there appears to be a robust effect of Abem on HEC-1-AR tumor weight. Can the authors explain this effect in resistant cells?

Response to Reviewer: We thank the Reviewer for pointing out this issue. Compared with the control group, treatment of Abemaciclib alone slightly attenuated the tumor growth and suppress tumor weight but the data did not reach the statistical significance (Fig. 7B, **Response Figure 22**). The data are shown as follows and provided in the Source Data file.

Response Figure 22

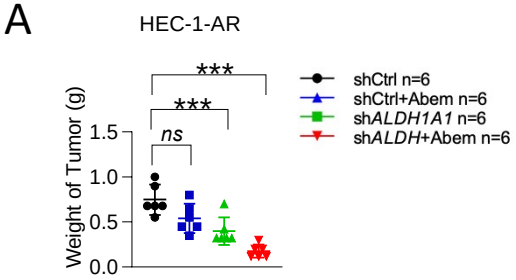

Response Figure 22. (A) Weight of tumors with shCtrl, sh*ALDH1A1*, Abemaciclib, or combination in HEC-1-AR xenografts, error bars represent ± SD.

7) Supplementary Fig. 5C: Levels of cyclin D1 protein should be shown.
Response to Reviewer: We thank the advice from the Reviewer. Levels of cyclin D1 protein have been examined using WB and the results have been shown in the Supplementary Fig. 5H (**Response Figure 23**).

Response Figure 23

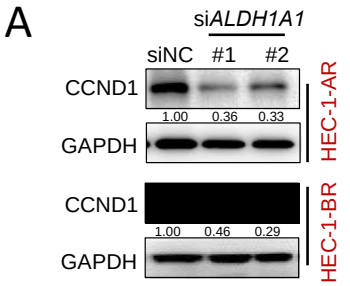

Response Figure 23. (A) Immunoblot analysis of CCND1 and GAPDH in HEC-1-AR and HEC-1-BR cells transfected with siNC or si*ALDH1A1*.

References

1. B. Langmead, S. L. Salzberg, Fast gapped-read alignment with Bowtie 2. *Nat Methods* **9**, 357-359 (2012).
2. H. Li *et al.*, The Sequence Alignment/Map format and SAMtools. *Bioinformatics* **25**, 2078-2079 (2009).
3. J. Feng, T. Liu, B. Qin, Y. Zhang, X. S. Liu, Identifying ChIP-seq enrichment using MACS. *Nat Protoc* **7**, 1728-1740 (2012).
4. W. A. Whyte *et al.*, Master transcription factors and mediator establish super-enhancers at key cell identity genes. *Cell* **153**, 307-319 (2013).
5. S. Heinz *et al.*, Simple combinations of lineage-determining transcription factors prime cis-regulatory elements required for macrophage and B cell identities. *Mol Cell* **38**, 576-589 (2010).
6. F. Ramirez, F. Dundar, S. Diehl, B. A. Gruning, T. Manke, deepTools: a flexible platform for exploring deep-sequencing data. *Nucleic Acids Res* **42**, W187-191 (2014).
7. H. Thorvaldsdottir, J. T. Robinson, J. P. Mesirov, Integrative Genomics Viewer (IGV): high-performance genomics data visualization and exploration. *Brief Bioinform* **14**, 178-192 (2013).
8. A. Dutta, T. Sen, A. Chatterjee, All-trans retinoic acid (ATRA) downregulates MMP-9 by modulating its regulatory molecules. *Cell Adh Migr* **4**, 409-418 (2010).
9. T. Liu *et al.*, CPSF6-RARgamma interacts with histone deacetylase 3 to promote myeloid transformation in RARG-fusion acute myeloid leukemia. *Nat Commun* **16**, 616 (2025).
10. A. De Simone *et al.*, Discovery of the First-in-Class GSK-3beta/HDAC Dual Inhibitor as Disease-Modifying Agent To Combat Alzheimer's Disease. *ACS Med Chem Lett* **10**, 469-474 (2019).
11. Y. Wang *et al.*, Discovery of novel glycogen synthase kinase-3alpha inhibitors: Structure-based virtual screening, preliminary SAR and biological evaluation for treatment of acute myeloid leukemia. *Eur J Med Chem* **171**, 221-234 (2019).
12. N. Cabezas-Wallscheid *et al.*, Vitamin A-Retinoic Acid Signaling Regulates Hematopoietic Stem Cell Dormancy. *Cell* **169**, 807-823 e819 (2017).
13. M. Colucci *et al.*, Retinoic acid receptor activation reprograms senescence response and enhances anti-tumor activity of natural killer cells. *Cancer Cell* **42**, 646-661 e649 (2024).
14. J. Galvao *et al.*, Unexpected low-dose toxicity of the universal solvent DMSO. *FASEB J* **28**, 1317-1330 (2014).
15. W. E. Glaab *et al.*, Characterization of distinct human endometrial carcinoma cell lines deficient in mismatch repair

that originated from a single tumor. *J Biol Chem* **273**, 26662-26669 (1998).
16. L. W. Francis *et al.*, Progesterone induces nano-scale molecular modifications on endometrial epithelial cell surfaces. *Biol Cell* **101**, 481-493 (2009).
17. M. J. Presta M, Rusnati M, Moscatelli D, Ragnotti G., Modulation of plasminogen activator activity in human endometrial adenocarcinoma cells by basic fibroblast growth factor and transforming growth factor beta. *Cancer Research* **15**, 6384-6389 (1988).
18. K. A. Kilowski *et al.*, KRAS mutations in endometrial cancers: Possible prognostic and treatment implications. *Gynecol Oncol* **191**, 299-306 (2024).
19. N. Cancer Genome Atlas Research *et al.*, Integrated genomic characterization of endometrial carcinoma. *Nature* **497**, 67-73 (2013).
20. Z. Li *et al.*, Loss of the FAT1 Tumor Suppressor Promotes Resistance to CDK4/6 Inhibitors via the Hippo Pathway. *Cancer Cell* **34**, 893-905 e898 (2018).
21. H. M. Lei *et al.*, Aldehyde dehydrogenase 1A1 confers erlotinib resistance via facilitating the reactive oxygen species-reactive carbonyl species metabolic pathway in lung adenocarcinomas. *Theranostics* **9**, 7122-7139 (2019).
22. K. Lavudi, S. M. Nuguri, P. Pandey, R. R. Kokkanti, Q. E. Wang, ALDH and cancer stem cells: Pathways, challenges, and future directions in targeted therapy. *Life Sci* **356**, 123033 (2024).
23. S. Tian, D. H. Liu, D. Wang, F. Ren, P. Xia, Aldehyde Dehydrogenase 1 (ALDH1) Promotes the Toxicity of TRAIL in Non-Small Cell Lung Cancer Cells via Post-Transcriptional Regulation of MEK-1 Expression. *Cell Physiol Biochem* **51**, 217-227 (2018).
24. Y. D. Ziyang Wang, Xiangqiong Wen, Ye Liu, Lvlan Ye, Xiang Zhang, Jiale Qin, upeng Wang, Huiying Chu, Guohui Li, Weijing Zhang, Xiongjun Wang, Weiling He, NIT2 dampens BRD1 phase separation and restrains. *Science Translational Medicine* **16** (2024).
25. J. M. Hsu *et al.*, MTAP deficiency confers resistance to cytosolic nucleic acid sensing and STING agonists. *Science* **390**, ead14089 (2025).
26. F. L. Yingyi Liu , Jie Liu, Dongzhi Cairang, Xiaomian Li, Peng Xia, Weijie Ma, Tiangen Wu, Xiangdong Gongye, Zhonglin Zhang, Xi Chen, Wenzhi He, Yufeng Yuan, The Acetyltransferase ARD1 Induces Glutathione Synthesis to Facilitate. *Cancer research* **85**, 4212-4232 (2025).
27. B. C. Guangyang Han, Michael J. Connor, Neil Sidell, Enhanced potency of 9-cis versus all-trans-retinoic acid to induce the

differentiation of human neuroblastoma cells. *Differentiation* **59**, 61-69 (1995).
28. N. Bayeva, E. Coll, O. Piskareva, Differentiating Neuroblastoma: A Systematic Review of the Retinoic Acid, Its Derivatives, and Synergistic Interactions. *J Pers Med* **11** (2021).
29. U. Testa, G. Castelli, E. Pelosi, Recent Developments in Differentiation Therapy of Acute Myeloid Leukemia. *Cancers (Basel)* **17** (2025).
30. K. M. Ferguson *et al.*, Palbociclib releases the latent differentiation capacity of neuroblastoma cells. *Dev Cell* **58**, 1967-1982 e1968 (2023).
31. L. Hu *et al.*, The CDK4/6 Inhibitor Palbociclib Synergizes with ATRA to Induce Differentiation in AML. *Mol Cancer Ther* **23**, 961-972 (2024).
32. Y. Yokoyama *et al.*, BET Inhibitors Suppress ALDH Activity by Targeting ALDH1A1 Super-Enhancer in Ovarian Cancer. *Cancer Res* **76**, 6320-6330 (2016).
33. X. Yao *et al.*, VHL Deficiency Drives Enhancer Activation of Oncogenes in Clear Cell Renal Cell Carcinoma. *Cancer Discov* **7**, 1284-1305 (2017).
34. S. W. Jingfeng Zhou, Danian Nie, Peilong Lai, Yiqing Li,, Y. J. Yangqiu Li, Jingxuan Pan, Super-enhancer landscape reveals leukemia stem cell reliance on X-box binding protein 1 as a therapeutic vulnerability. *SCIENCE TRANSLATIONAL MEDICINE* **13** (2021).
35. R. Li *et al.*, Super-enhancer RNA m(6)A promotes local chromatin accessibility and oncogene transcription in pancreatic ductal adenocarcinoma. *Nat Genet* **55**, 2224-2234 (2023).
36. S. Xiong *et al.*, Super enhancer acquisition drives expression of oncogenic PPP1R15B that regulates protein homeostasis in multiple myeloma. *Nat Commun* **15**, 6810 (2024).
37. Y. Y. Jiang *et al.*, Targeting super-enhancer-associated oncogenes in oesophageal squamous cell carcinoma. *Gut* **66**, 1358-1368 (2017).
38. N. D. Heintzman *et al.*, Histone modifications at human enhancers reflect global cell-type-specific gene expression. *Nature* **459**, 108-112 (2009).
39. N. D. Heintzman *et al.*, Distinct and predictive chromatin signatures of transcriptional promoters and enhancers in the human genome. *Nat Genet* **39**, 311-318 (2007).
40. S. Chen *et al.*, Activation of epigenetic reprogramming via crotonylation overcomes resistance to EGFR-TKI therapy in lung cancer. *Proc Natl Acad Sci U S A* **122**, e2509255122 (2025).

41. V. Wagner, J. Gil, Senescence as a therapeutically relevant response to CDK4/6 inhibitors. *Oncogene* **39**, 5165-5176 (2020).
42. N. M. Kettner *et al.*, Combined Inhibition of STAT3 and DNA Repair in Palbociclib-Resistant ER-Positive Breast Cancer. *Clin Cancer Res* **25**, 3996-4013 (2019).
43. C. Costa *et al.*, PTEN Loss Mediates Clinical Cross-Resistance to CDK4/6 and PI3Kalpha Inhibitors in Breast Cancer. *Cancer Discov* **10**, 72-85 (2020).
44. Z. Cai *et al.*, Overexpressed Cyclin D1 and CDK4 proteins are responsible for the resistance to CDK4/6 inhibitor in breast cancer that can be reversed by PI3K/mTOR inhibitors. *Sci China Life Sci* **66**, 94-109 (2023).
45. V. Kumarasamy *et al.*, RB loss determines selective resistance and novel vulnerabilities in ER-positive breast cancer models. *Oncogene* **41**, 3524-3538 (2022).
46. Z. F. Xianbing Zhu, Kendall Dutchak, Azadeh Arabzadeh, Simon Milette, Jutta, G. M. Steinberger, Anie Monast, Virginie Pilon, Tim Kong, Bianca N, E. P. M. Adams, Hannah JB Hosein, Tianxu Fang, Jing Su, Yibo Xue,, V. S. Roni Rayes, Logan A Walsh, Guojun Chen, Daniela F Quail,, M. P. Jonathan D Spicer, David Dankort, Sidong Huang, Co-targeting CDK4 6 and BRD4 promotes senescence and ferroptosis sensitivity in cancer. *Cancer research* **84**, 1333 - 1351 (2024).
47. Y. Zhang *et al.*, Discovery of dual CDK4/6 and BRD4 inhibitor as apoptosis and autophagy inducers against NSCLC in vitro and in vivo. *Eur J Med Chem* **290**, 117495 (2025).
48. C. Wu *et al.*, PARP and CDK4/6 Inhibitor Combination Therapy Induces Apoptosis and Suppresses Neuroendocrine Differentiation in Prostate Cancer. *Mol Cancer Ther* **20**, 1680-1691 (2021).
49. Y. Wen *et al.*, CDK4/6 Inhibitors Impede Chemoresistance and Inhibit Tumor Growth of Small Cell Lung Cancer. *Adv Sci (Weinh)* **11**, e2400666 (2024).
50. R. Kudo *et al.*, Long-term breast cancer response to CDK4/6 inhibition defined by TP53-mediated geroconversion. *Cancer Cell* 10.1016/j.ccell.2024.09.009 (2024).
51. F. Dang *et al.*, Inhibition of CK1epsilon potentiates the therapeutic efficacy of CDK4/6 inhibitor in breast cancer. *Nat Commun* **12**, 5386 (2021).
52. Q. Li *et al.*, INK4 Tumor Suppressor Proteins Mediate Resistance to CDK4/6 Kinase Inhibitors. *Cancer Discov* **12**, 356-371 (2022).
53. E. S. Knudsen *et al.*, Cell cycle plasticity driven by MTOR signaling: integral resistance to CDK4/6 inhibition in patient-derived models of pancreatic cancer. *Oncogene* **38**, 3355-3370 (2019).

54. Z. Q. Wang *et al.*, Bromodomain and extraterminal (BET) proteins: biological functions, diseases, and targeted therapy. *Signal Transduct Target Ther* **8**, 420 (2023).

Response Letter to Research Article-NCOMMS-25-43591A

KEY:

BLACK TEXT: Editor comments

BLUE TEXT: Author responses

RED TEXT: Changes made to text in manuscript

****

REVIEWER COMMENTS

Reviewer #1 (Remarks to the Author):

The authors have revised their manuscript in response to the reviewers' suggestions, and several aspects have improved. Nonetheless, some points remain that require clarification or further detail.

Response to Reviewer: We appreciate the positive comments from the Reviewer. We believe that we have fully addressed all the concerns in the point-by-point responses below.

Response to comment 1 and 2:
The methodological description used to determine the IC50 values in Fig. 1C and the Response Fig. 1A requires some further clarification in the Methods section. Based on the graphs, we assume that PDOs were exposed to the drug concentrations indicated on the y-axis, however this should be stated somewhere. In addition, we could not find information on "MAcreGel" and Mingao Biotech.

We appreciate the inclusion of the new data on Palbociclib and Ribociclib. It would be important to clarify whether these experiments were performed in parallel with the Abemaciclib treatments. The striking similarity of the responses raises the question whether the PDOs display a general, non-specific sensitivity or reduced survival capability rather than a selective response to the individual CDK4/6 inhibitors. It may be worth testing additional more monospecific CDK inhibitors, since this could help disentangle compound specific from general CDK related effects. Some work already exists that investigates the synergistic effects of ATRA with CDK inhibitors of different specificity, including ryuvidine and more selective CDK4 inhibitors.

Response to Reviewer: We thank the Reviewer for pointing out these issues. The sensitivity of 16 EC PDOs to CDK4/6 inhibitors was assessed by generating dose-response curves across a range of concentrations, including Abemaciclib (0, 0.1, 0.5, 1, 2.5, 10, 25, or 50 μM), Palbociclib (0, 0.1, 0.5, 2.5, 5, 12.5, 25, or 50 μM) and Ribociclib (0, 0.1, 0.5, 2.5, 5, 12.5, 25, or 50 μM). Dose-response curves were generated by plotting relative viability against the logarithm of drug concentration. The curves were

fitted by nonlinear regression using a sigmoidal dose–response model (variable slope) in GraphPad Prism 9.0. Under this model, the half-maximal inhibitory concentration (IC50) was defined as the drug concentration that reduced cell viability to 50% of the vehicle control value, as derived from the fitted dose–response curves. We have presented the dose-response curves of 16 EC PDOs, which could clearly demonstrate the differences in the sensitivity of these PDOs to CDK4/6 inhibitors (**Response Figure 1A-C**). We have amended the description of the methodology used to determine the IC50 values of PDOs in the Method section. The bar graph showed the IC50 values of Abemaciclib, Palbociclib, and Ribociclib across a panel of 16 EC PDOs, which have been stated in the updated Methods section and figure legends.

We apologized for the missing of information on "MAcreGel" and Mingao Biotech. The detailed information (#120231, Mingao Biotech, Shenzhen, China) is available at http://www.mingaobio.com/ProductDetail/10191141.html, and this has been amended in the updated version.

Actually, the IC50 experiments using different CDK4/6 inhibitors (Abemaciclib, Palbociclib, and Ribociclib) across the 16 EC PDOs were conducted under parallel experimental conditions. This point was clarified in the revised Methods section. The reason for the similarity of the responses of these inhibitors to cancer cells may be that Abemaciclib, Palbociclib and Ribociclib are all highly specific inhibitors of CDK4/6. Of note, some PDOs exhibited varying degrees of sensitivity to different CDK4/6i, such as PDO53 and PDO65, which showed more resistance to Abemaciclib (PDO53-IC50: 1.97 μM, PDO65-IC50: 7.43 μM) or Palbociclib (PDO53-IC50: 7.00 μM, PDO65-IC50: 11.68 μM) than to Ribociclib (PDO53-IC50: 5.22 μM, PDO65-IC50: 9.30 μM) (**Response Figure 1A-C**).

To further clarify whether the similarity in sensitivity to different CDK4/6 inhibitors of PDOs is attributable to non-specific effects, we conducted the IC50 experiments using another monospecific CDK4 inhibitor Ryuvidine across the panel of 16 EC PDOs. The inhibitor exhibited a different growth inhibition trend compared to those observed with the CDK4/6i (**Response Figure 1D**), suggesting that these PDOs displayed a selective response to CDK4/6i rather than a general sensitivity to CDK inhibitors. Thus, the broadly similar responses of these PDOs to the three drugs may be due to their common mechanism of action.

Furthermore, we appreciate the Reviewer for pointing out the differential effects of ATRA combined with CDK inhibitors in different cancer types, the underlying mechanisms are interesting and warrant further investigation in the further work.

In Method section (Page 23-24):

"For organoid culture, tumor tissue was dissociated into small pieces and digested with collagenase II (2 mg/mL) and collagenase IV (2 mg/mL) for 30 min at 37°C. Following digestion, the mixture was filtered through a 70-μm cell strainer to remove large undigested fragments. The isolated cells were plated in ice-cold MAcreGel (#120231, Mingao Biotech, Shenzhen, China) in six-well culture plates. After allowing the MAcreGel drops to solidify for 15 min at 37°C, cells were overlaid with endometrial cancer organoid medium, composed of Ad-DF+++ supplemented with 1× O-27

supplement (#R1210, Mingao Biotech, Shenzhen, China), 100 ng/mL recombinant human Noggin (120-10C, Peprotech), 250 ng/mL recombinant human R-spondin-1 (120-38, Peprotech), 1.25 mM N-acetylcystein (A9165, Sigma-Aldrich), 10 mM nicotinamide (N0636, Sigma-Aldrich), 50 ng/mL human recombinant EGF (AF-100-15, Peprotech), 100 ng/mL human recombinant FGF-10 (100-26, Peprotech), 500 nM A83-01 (No.2939, Tocris), 100 nM SB202190 (S1077, Selleck), 10 nM β-estradiol (HY-B0141, MedChemExpress) and 10 μM Y-27632 (M20999, AbMole). Organoids were routinely passaged by dissociation using TrypLE™ Express (Gibco, 12604013) for 10 min at 37°C.

For the cell viability assay, organoids were harvested and dissociated using TrypLE™ Express (Gibco, 12604013) for 10 min at 37 ºC. The dissociated PDOs were resuspended in ice-cold MAcreGel (#120231, Mingao Biotech, Shenzhen, China) and seeded into a 96-well plate (Corning). After allowing the MAcreGel drops to solidify for 15 min at 37 ºC, PDOs were overlaid with endometrial cancer organoid medium containing the indicated doses of drugs, including Abemaciclib (0, 0.1, 0.5, 1, 2.5, 10, 25, or 50 μM), Palbociclib (0, 0.1, 0.5, 2.5, 5, 12.5, 25, or 50 μM), and Ribociclib (0, 0.1, 0.5, 2.5, 5, 12.5, 25, or 50 μM). DMSO-treated wells corresponding to the drug treatment groups served as the vehicle control (100% viability). Five days after drug treatment, cell viability was measured using the 3D Cell Viability ATP Assay Kit (#R1101, Mingao Biotech, Shenzhen, China) according to the manufacturer's instructions on a Spark microplate reader (Tecan). The ATP values were normalized to vehicle control (set as 100%) to calculate the relative viability (%) for each well. Dose-response curves were generated by plotting relative viability against the logarithm of drug concentration. The curves were fitted by nonlinear regression using a sigmoidal dose–response model (variable slope) in GraphPad Prism 9.0. Under this model, the half-maximal inhibitory concentration (IC50) is defined as the drug concentration that reduced cell viability to 50% of the vehicle control value. IC50 values were derived from the fitted dose–response curves. The drug treatments (Abemaciclib, Palbociclib, and Ribociclib) across the 16 EC PDOs were conducted in parallel experimental conditions."

In Figure Legend (Page 40): "(C) Sensitivity of 16 EC PDOs to Abemaciclib. Bar graph showing the half-maximal inhibitory concentration (IC50) values of Abemaciclib across a panel of 16 EC PDOs. IC50 values were derived from dose-response curves."

In Supplementary Figure Legend: "(A-B) Sensitivity of 16 EC PDOs to Palbociclib and Ribociclib. Bar graph shows the IC50 values of Palbociclib (A) and Ribociclib (B) across a panel of 16 EC PDO lines. IC50 values were derived from dose-response curves."

Response Figure 1

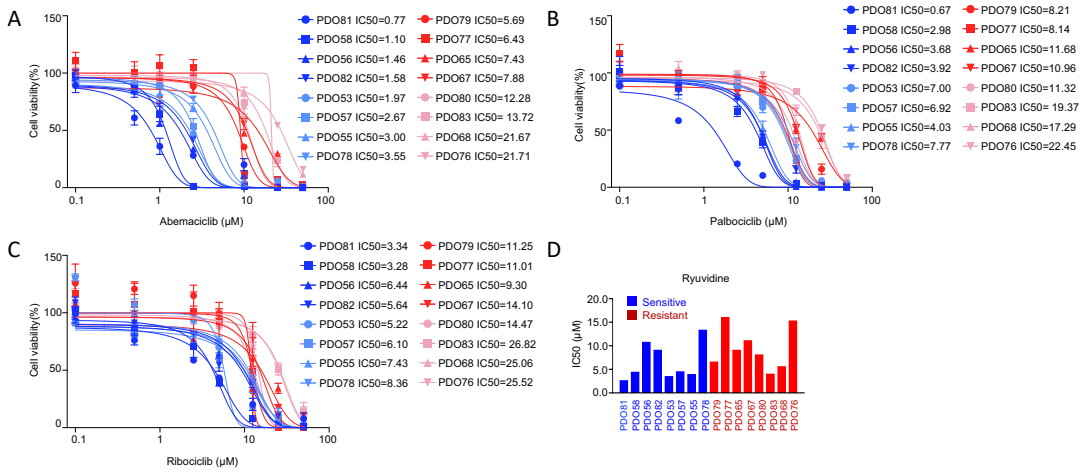

Response Figure 1. (A-C) Sensitivity of 16 EC PDOs to three CDK4/6 inhibitors. Cell viability is determined upon five days of treatment and normalized to vehicle control. The IC50 values are shown. (A) Abemaciclib. (B) Palbociclib. (C) Ribociclib. (D) Sensitivity of 16 EC PDOs to Ryuvidine. Bar graph showing the half-maximal inhibitory concentration (IC50) values of Ryuvidine across a panel of 16 EC PDOs. IC50 values were derived from dose-response curves.

Response to comment 5:

Regarding the ATRA concentrations used, we would like to note that pharmacokinetic studies in patients with APL indicate that the clinically applied doses result in peak plasma levels of approximately 1 µM ATRA. In our experience, concentrations as low as 10 nM ATRA can already influence RAR reporter assays. In the manuscript cited by the authors stating: "10–30 µM RA was used in HL60 and NB4 cells (11)", one can see that although concentrations up to 30 µM were tested, 1 µM already caused the major effects on cell viability.

We therefore asked whether a concentration of 20 µM is still specific for ATRA mediated activation and transmitted by retinoic acid receptors or whether such a dose might induce additional, non specific effects, including increased expression of ALDH1A1.

Is a higher concentration required for RAR reporter activity in this particular cell type, and what would be the mechanistic explanation? How can peak plasma levels of 20 µM ATRA be reached in patients? How do other cell lines respond? Are the observed effects cell type specific? If so, we would suggest reflecting this in the title of the manuscript.

Response to Reviewer: We thank the Reviewer for raising these issues regarding the 20 µM RA dose used in this study. To investigate whether a concentration of 20 µM is still specific for RA mediated activation and transmitted by retinoic acid receptor (RAR), we treated HEC-1-B cells with increasing concentrations of RA (1, 5, 20 µM) and found that the expression levels of *ALDH1A1* were elevated in a dose-dependent

manner, and this effect could be significantly abrogated by the knockdown of RARα via siRNA-mediated silencing (**Response Figure 2A**). These results indicated that RA exerted its biological effects in a dose-dependent manner in EC cells, and the effect of 20 μM RA treatment was still dependent on RARα rather than non-specific activity.

To investigate the effects of RA concentrations on RAR activity, we performed RAR reporter assays using luciferase reporter plasmids (RAR-luc) as previously reported (1) in various cancer cell lines, including endometrial cancer cells HEC-1-A/B, breast cancer cells MCF7 and T47D, and colorectal cancer cells HCT116 and RKO. We treated these cells with increasing dosages of RA and demonstrated that distinct cell lines exhibit different sensitivity to RA (**Response Figure 2B**). Specifically, all cell lines exhibited varying degrees of RAR activation at 20 μM RA, with RAR activity further increasing in a dose-dependent manner upon RA escalation; notable divergence in response kinetic profiles was observed among different cell lines (**Response Figure 2B**). These findings indicate cell-type-specific RA responses, potentially attributed to differential RAR expressions, as reported by previous studies (2-4), with specific mechanisms pending further study.

We appreciate the comment from the Reviewer that the clinically applied dose of RA is approximately 1 μM. Numerous studies showed that following a 45 mg/m^2 oral dose of RA in patients, peak plasma concentrations range from 0.1 to 8 μM, with a median peak concentration of approximately 1 μM.(5) Thus, such a high concentration of 20 μM RA may be difficult to achieve in clinic. Furthermore, our data showed that the effects of RA are dose-dependent to induce *ALDH1A1* expression and antagonize the anti-tumor effect of Abemaciclib, which exhibited the significant effect in 1 μM or 20 μM of RA treatment (**Response Figure 2C-E**). We agree with the reviewer's suggestion that 1 μM RA is more clinically relevant. Thus, we have conducted all experiments originally conducted at 20 μM RA using 1 μM RA (**Response Figure 3**), and the results confirmed that 1 μM RA elicits equivalent biological effects to 20 μM RA. Consequently, we have replaced all data generated with 20 μM RA in the Main Figures with those obtained at the clinically relevant concentration of 1 μM RA, retaining only the data regarding the dose-dependent effects of RA on *ALDH1A1* expression and cell viability under CDK4/6i treatment in Supplemental Figure 6.

Given that we only validated the ALDH1A1-RARα/ERα axis in ER-positive tumors without confirming this mechanism in other tumor types, we revised the article title in the updated version in accordance with the reviewers' comments as follows:

"Targeting Super-Enhancer-Driven ALDH1A1-RARα/ERα Feedback Loop to Mitigate CDK4/6 Inhibitor Resistance via Suppression of Vitamin A Metabolism in ER-Positive Cancers".

Response Figure 2

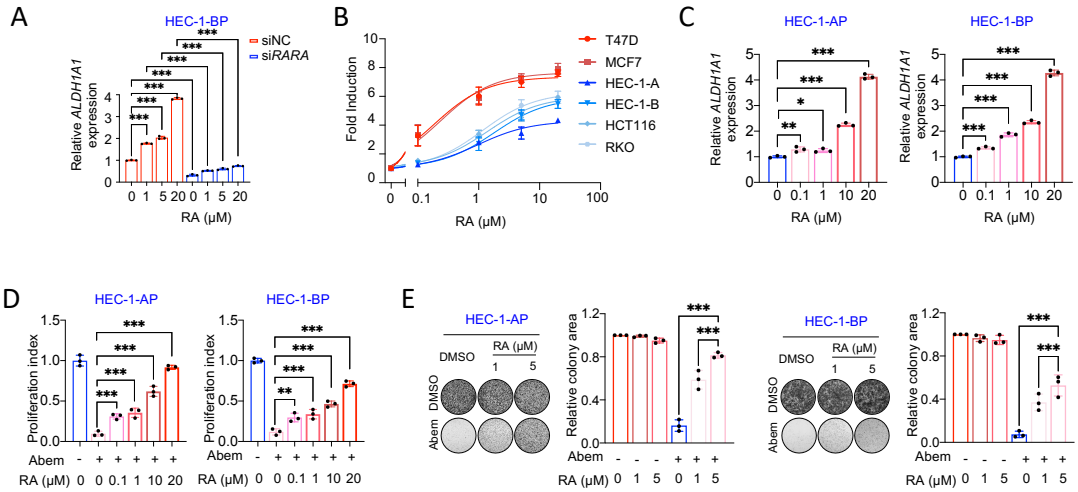

Response Figure 2. (A) RT-qPCR validation of *ALDH1A1* in HEC-1-BP cells treated with DMSO, RA (1 μM, 5μM and 20 μM). Data are shown as mean ± SD and analyzed by one-way ANOVA with Dunnett's multiple comparisons test. (B) RAR reporter assays in various cancer cell lines. Cells were co-transfected with a RAR-luc reporter and pRL-TK plasmids for 24 h and then treated with indicated doses of RA. Cell lysates were subjected to luciferase activity assays using the dual luciferase reporter assay system, and the luciferase activity was normalized to pRL-TK activity. (C) RT-qPCR validation of *ALDH1A1* in HEC-1-AP cells treated with DMSO, RA (0.1 μM, 1 μM, 10 μM or 20 μM). Data are shown as mean ± SD and analyzed by one-way ANOVA with Dunnett's multiple comparisons test. (D) Proliferation index of HEC-1-AP and HEC-1-BP cells. Cells were treated with combinations of RA (0 μM, 0.1 μM, 1 μM, 10 μM or 20 μM) and Abemaciclib (0.5 μM). The number of viable cells is measured at 96 hours. Data are shown as mean ± SD and analyzed by one-way ANOVA with Dunnett's multiple comparisons test. (E) Representative images of colony formation assay in parental cells (HEC-1-AP and HEC-1-BP) treated with DMSO, RA (1 or 5 μM), Abemaciclib (0.5 μM), or combination. Data are shown as mean ± SD of three independent experiments and analyzed by one-way ANOVA with Dunnett's multiple comparisons test. ns, not significant, $*p < 0.05$, $**p < 0.01$, $***p < 0.001$.

Response Figure 3

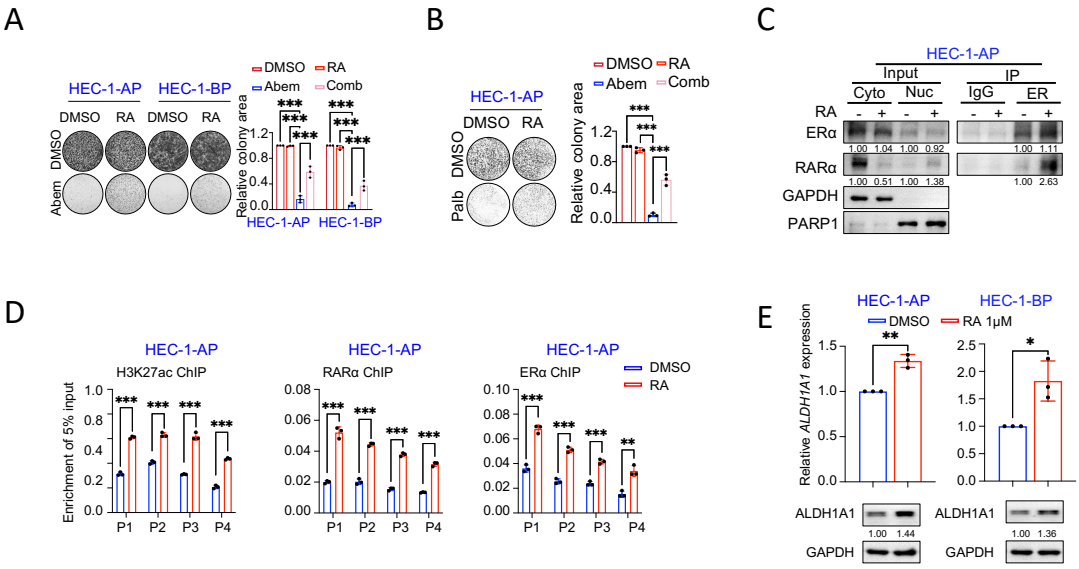

Response Figure 3. (A) Representative images and quantification of colony formation assay in parental cells (HEC-1-AP and HEC-1-BP) treated with DMSO, RA (1 μM), Abemaciclib (0.5 μM), or combination. Data are shown as mean ± SD of three independent experiments and analyzed by One-way ANOVA with Dunnett's multiple comparisons test. ***$p < 0.001$. (B) Representative images and quantification of colony formation assay of HEC-1-AP cells treated with DMSO, RA (1 μM), Palbociclib (0.5 μM), or combination. Data are shown as mean ± SD of three independent experiments and analyzed by One-way ANOVA with Dunnett's multiple comparisons test. ***$p <$ 0.001. (C) Immunoblot analysis of ERα and RARα in nucleus of HEC-1-AP cells treated with DMSO and RA (1 μM) for 72 hours. Co-IP shows the interaction of ERα and RARα in HEC-1-AP cells treated with DMSO and RA (1 μM) for 72 hours. (D) ChIP qPCR analysis of H3K27ac, ERα and RARα occupancy at genomic loci of *ALDH1A1* in HEC-1-AP cells treated with DMSO and RA (1 μM) for 72 hours. Data are presented relative to input, shown as mean ± SD of three independent experiments and analyzed by unpaired t-test. **$p < 0.01$, ***$p < 0.001$. (E) RT-qPCR validation of *ALDH1A1* in HEC-1-AP and HEC-1-BP cells treated with DMSO or RA (1 μM). Data are shown as mean ± SD of three independent experiments and analyzed by t test. *$p <$ 0.05, **$p < 0.01$. (up). Immunoblot analysis of ALDH1A1 in HEC-1-AP and HEC-1-BP cells treated with RA (1 μM) for 72 hours (down).

Response to comment 8:

It may be helpful to rename the primer sets (P1–4) to improve clarity. In addition, ALDH1A1 should be mentioned in the figure.

Response to Reviewer: We thank the constructive advice from the Reviewer. To clarify the observed effects, we have amended the figure in the updated version as follow (**Response Figure 4**). We have supplemented the following description in the main text (Page 8): "To determine the differential levels of H3K27ac across the ALDH1A1 regions, we designed four sets of primers (P1-P4) for ChIP-qPCR analysis."

Response Figure 4

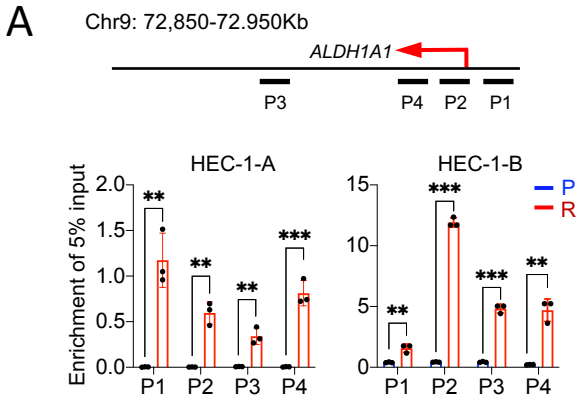

Response Figure 4. (A) Schematic diagram of the ChIP primers (P1–P4) locations across the ALDH1A1 region (upper). ChIP-qPCR analysis of H3K27ac occupancy at genomic loci of *ALDH1A1* (P1-4) in parental (P) and resistant (R) cells (bottom). Data are presented relative to input, shown as mean ± SD of three independent experiments and analyzed by unpaired t-test. $^{**}p < 0.01$, $^{***}p < 0.001$.

Reviewer #2 (Remarks to the Author):

I co-reviewed this manuscript with one of the reviewers who provided the listed reports. This is part of the Nature Communications initiative to facilitate training in peer review and to provide appropriate recognition for Early Career Researchers who co-review manuscripts.

Response to Reviewer: We highly appreciate the ECR co-review program. We thank the Reviewer for the positive comments and constructive suggestions.

References

1. B. Dai *et al.*, Targeting HDAC3 to overcome the resistance to ATRA or arsenic in acute promyelocytic leukemia through ubiquitination and degradation of PML-RARalpha. *Cell Death Differ* **30**, 1320-1333 (2023).
2. R. N. R. Valentine B Andela The proteosome inhibitor MG132 attenuates Retinoic Acid. *Molecular Cancer* **3** (2004).
3. J. H. Shi, B. Zheng, S. Chen, G. Y. Ma, J. K. Wen, Retinoic acid receptor alpha mediates all-trans-retinoic acid-induced Klf4 gene expression by regulating Klf4 promoter activity in vascular smooth muscle cells. *J Biol Chem* **287**, 10799-10811 (2012).
4. J. De-Castro Arce *et al.*, Ectopic expression of nonliganded retinoic acid receptor beta abrogates AP-1 activity by selective degradation of c-Jun in cervical carcinoma cells. *J Biol Chem* **279**, 45408-45416 (2004).
5. P. C. ADAMSON, All-Trans-Retinoic Acid Pharmacology and Its Impact on the Treatment of Acute Promyelocytic Leukemia. *Oncologist* **1**, 305-314 (1996).